LIÈGE université Library

https://lib.uliege.be

https://matheo.uliege.be

Mémoire

Auteur : Martin, Samuel
Promoteur(s) : Alvera Azcarate, Aida; 14938
Faculté : Faculté des Sciences
Diplôme : Master en océanographie, à finalité approfondie
Année académique : 2020-2021
URI/URL : http://hdl.handle.net/2268.2/12866

Avertissement à l'attention des usagers :

Tous les documents placés en accès ouvert sur le site le site MatheO sont protégés par le droit d'auteur. Conformément aux principes énoncés par la "Budapest Open Access Initiative"(BOAI, 2002), l'utilisateur du site peut lire, télécharger, copier, transmettre, imprimer, chercher ou faire un lien vers le texte intégral de ces documents, les disséquer pour les indexer, s'en servir de données pour un logiciel, ou s'en servir à toute autre fin légale (ou prévue par la réglementation relative au droit d'auteur). Toute utilisation du document à des fins commerciales est strictement interdite.

Par ailleurs, l'utilisateur s'engage à respecter les droits moraux de l'auteur, principalement le droit à l'intégrité de l'oeuvre et le droit de paternité et ce dans toute utilisation que l'utilisateur entreprend. Ainsi, à titre d'exemple, lorsqu'il reproduira un document par extrait ou dans son intégralité, l'utilisateur citera de manière complète les sources telles que mentionnées ci-dessus. Toute utilisation non explicitement autorisée ci-avant (telle que par exemple, la modification du document ou son résumé) nécessite l'autorisation préalable et expresse des auteurs ou de leurs ayants droit.

LIÈGE université

GHER GeoHydrodynamics & Environment Research

museum Operational Directorate Natural Environment
OD Nature | OD Natuur | DO Nature

EUTROPHICATION ASSESSMENT OF THE SOUTHERN NORTH SEA USING MULTI-SATELLITE DATASETS

Author : Samuel MARTIN

Supervisors : Aida ALVERA-AZCÁRATE (GHER) and Dimitry VAN DER ZANDE (RBINS)

A Thesis Submitted in Partial Fulfillment of the Requirements for the Master's Degree in Oceanography

University of Liège Faculty of Sciences Academic year 2020-2021

In accordance with the rules imposed on writing, this master thesis must not exceed 50 pages, written in Times 12 or equivalent.

Cover picture: composite satellite image of the southern North Sea captured on March 25 2020. The data were acquired by Moderate Resolution Imaging Spectroradiometer (MODIS) instruments on NASA's Terra and Aqua satellites (https://earthobservatory.nasa.gov/images/146556/a-sea-of-color-and-wind).

ACKNOWLEDGEMENTS

I would like to express my sincere thanks to my thesis director, Aida Alvera-Azcárate. I would like to thank her for introducing me to the world of satellite oceanography with wonder and for the beautiful pictures she shared with us during class. I thank her for listening to my research interests, which allowed me to find the ideal research topic. I thank her for all those meetings spent online, for her patience and for her valuable advices.

I would also like to thank Dimitry van der Zande for his expertise and involvement in this thesis. Your feedbacks were more than helpful.

I would also like to thank my girlfriend Alexandra, for having supported me all along the thesis, even from Spain, for her encouragement but also for having taken the time to listen to me when I doubted of myself.

My thanks also go to my parents. Thank you Mom for always pushing me hard into my studies. Thank you Dad for passing me your love of the ocean and nature since I was a kid. Thank you Ianna for your support. Thank you Mamy. Thank you to my two brothers and my friends for motivating me when I had doubts.

Finally, I would like to thank my grandfather for passing on his love of science and for having contributed to awaken my taste and curiosity for the world around us.

ABSTRACT

The North Sea (NS) is a highly productive semi-enclosed shelf sea of the Atlantic Ocean located in the northern Europe. The Southern North Sea (SNS), which is shallow and very well mixed, has long suffered from eutrophication problems. As a result, various policy measures have been taken by the NS surrounding countries (OSPAR Convention) with the aim of achieving good environmental status (GES) of the NS by 2020. The use of satellite remote sensing is a coherent method of data acquisition and provides information with generally much greater spatial and temporal coverage than in-situ data, which provide very localized information in space and time. Satellite remote sensing therefore offers an effective method to address long-term changes at the scale of an entire basin, such as the SNS. The main aim of this master thesis was to use high-level satellite gap-free products to assess the evolution of the eutrophication status and the phytoplankton dynamics of SNS over a period from 1998 to 2017.

Our analyses showed a strong gradient of chlorophyll concentrations (CHL, a proxy for phytoplankton biomass) from coastal areas (higher CHL) to offshore areas (lower CHL). At the scale of the SNS domain, CHL increased between 1998 - 2004, stagnated thereafter, until 2014, when it started to decrease, probably as a consequence of the reduction of river-bone nutrient inputs in the SNS. Our analyses also showed that the suspended particular matter concentration (SPM) increased over the period by 0.042 mg/L.year. In addition, sea surface temperature (SST) also increased by 0.021°C/year in the SNS, which is positively correlated to the North Atlantic Oscillation (NAO) over our period.

Another outcome is that we observed a phenological shift of about 1 month in the onset date of phytoplankton blooms. While it is difficult to identify a factor responsible for the observed phenological shift, it has been observed that the climate regime of the SNS changed during late 1990s. We therefore assume that this phenological shift is due to a change in planktonic communities associated with the rise in temperature as well as the de-eutrophication trend occurring in the SNS, which could have favored the emergence of winter diatom blooms.

RÉSUMÉ

La Mer du Nord (MN) est un mer continentale semi-fermée très productive de l'océan Atlantique, située au Nord-ouest de l'Europe. Le Sud de la Mer du Nord (SMN), qui est peu profond et fortement mélangé, a longtemps subi des problèmes d'eutrophisation. En conséquence, différentes mesures politiques ont été menées par les pays bordant la MN (convention OSPAR) dans le but d'obtenir, d'ici 2020, un bon état environnemental des eaux de la MN. Parmi les mesures adoptées, les pays de la convention OSPAR doivent réaliser une surveillance du niveau d'eutrophisation de leurs eaux. L'utilisation de la télédétection satellitaire est une méthode cohérente qui permet d'obtenir des informations avec une bien plus large couverture spatiale et temporelle que les mesures in-situ, qui nous donne qu'une information très localisée dans l'espace et dans le temps. La télédétection satellitaire offre donc une méthode efficace pour évaluer les changements à long-terme à l'échelle d'un bassin entier, comme celui du SMN. Ce mémoire de fin d'étude a donc eu pour but principal d'utiliser des produits satellitaires de haut niveau de traitement afin d'évaluer l'évolution du niveau d'eutrophisation ainsi que des dynamiques du phytoplancton dans le SMN sur une période s'étendant de 1998 à 2017.

Nos analyses ont montré un important gradient de concentration en chlorophylle (CHL, proxy de la biomasse phytoplanctonique) allant des zones côtières (CHL élevées) aux zones offshores (CHL plus faibles). À l'échelle de notre domaine, la CHL a augmenté entre 1998 - 2004, stagné ensuite, jusqu'en 2014, où elle a commencé à baisser, probablement en conséquence à la réduction de l'apport des nutriments par les voies fluviales. Nos analyses ont également montré que la concentration en matière en suspension (MES) avait augmenté au cours de la période à raison de 0.042 mg/L.an. De plus, la température de surface (TS) a également augmenté de 0.021°C/an dans le SMN.

Un autre résultat probant est que nous avons observé un shift phénologique d'environ 1 mois dans le déclenchement des blooms phytoplanctoniques entre 1998 et 2017. S'il est difficile d'identifier un facteur responsable de ce shift, il est à peu près certain que le régime climatique du SMN a changé au début de notre période. Nous pensons donc que ce shift phénologique est probablement dû à un changement des communautés planctoniques associé à la montrée des températures ainsi qu'à la tendance de dé-eutrophisation du SMN, qui auraient pu favoriser l'émergence de blooms hivernaux de diatomées.

TABLE OF CONTENTS

« The extent to which the suitability of water for its functional role in the biosphere or the human environment is determined by its optical properties » (Kirk, 1988)

CHAPTER I : INTRODUCTION

I.1. The North Sea

The North Sea (NS) is a semi-enclosed shelf sea of the Atlantic Ocean which has been formed by flooding during the Holocene (Ducrotoy & Elliott, 2008; Ducrotoy et al., 2000; Emeis et al., 2015). The NS is located in the northern Europe, between Great Britain, Shetland and Orkney islands, Norway, Denmark, Germany, the Netherlands, Belgium, and France and covers an area of approximately 575.000 km^2 (Otto et al., 1990). It is a typical large marine ecosystem which is connected to the ocean through the English Channel in the south and the through the Norwegian Sea in the north. It also receives low-salinity waters from the Baltic Sea through the Skagerrak and Kattegat, as well from continental rivers (Ducrotoy et al., 2000). Figure 1 shows a map of the North Sea with its bathymetry:

Figure 1 : map of the North Sea with its bathymery. Source: https://nl.m.wikipedia.org/wiki/Bestand:North_Sea_map-en.png

The NS basin is heavily sedimented, relatively shallow and deepens to the north (fig. 1) (Ducrotoy et al., 2000). Tides in the NS are strong and mainly semi-diurnal (Otto et al., 1990). In terms of bathymetry, the NS can be subdivided into the English Channel (with water depths varying from 50 – 100 m), the Southern North Sea (<50 m), the Central and Northern North Sea (~50 – 200 m) and the much deeper Norwegian trench (>200 m) (Ruddick et al., 2008). The basin has an average depth of 90 meters, and a maximum depth of 700 meters in the Norvegian Trench (Ducrotoy & Elliott, 2008; Ducrotoy et al., 2000). The northern and western coasts of the NS are mainly composed by rocky and mountainous shores, sandy beaches, or fjords, while the eastern the southern sides are mostly composed by sand beaches and dunes (Ducrotoy et al., 2000).

The NS is characterized by a broad connection to the Atlantic Ocean and by strong continental impacts coming from north-western European countries. This characteristic results in an interplay between oceanic influences (tides, the North Atlantic Oscillation and the North Atlantic Pressure system) and continental influences (freshwater discharges, heat fluxes and pollutants inputs) (Sündermann & Pohlmann, 2011). There is a great spatial heterogeneity in terms of oceanic and terrestrial influences, as seen in fig. 2 (Emeis et al., 2015) :

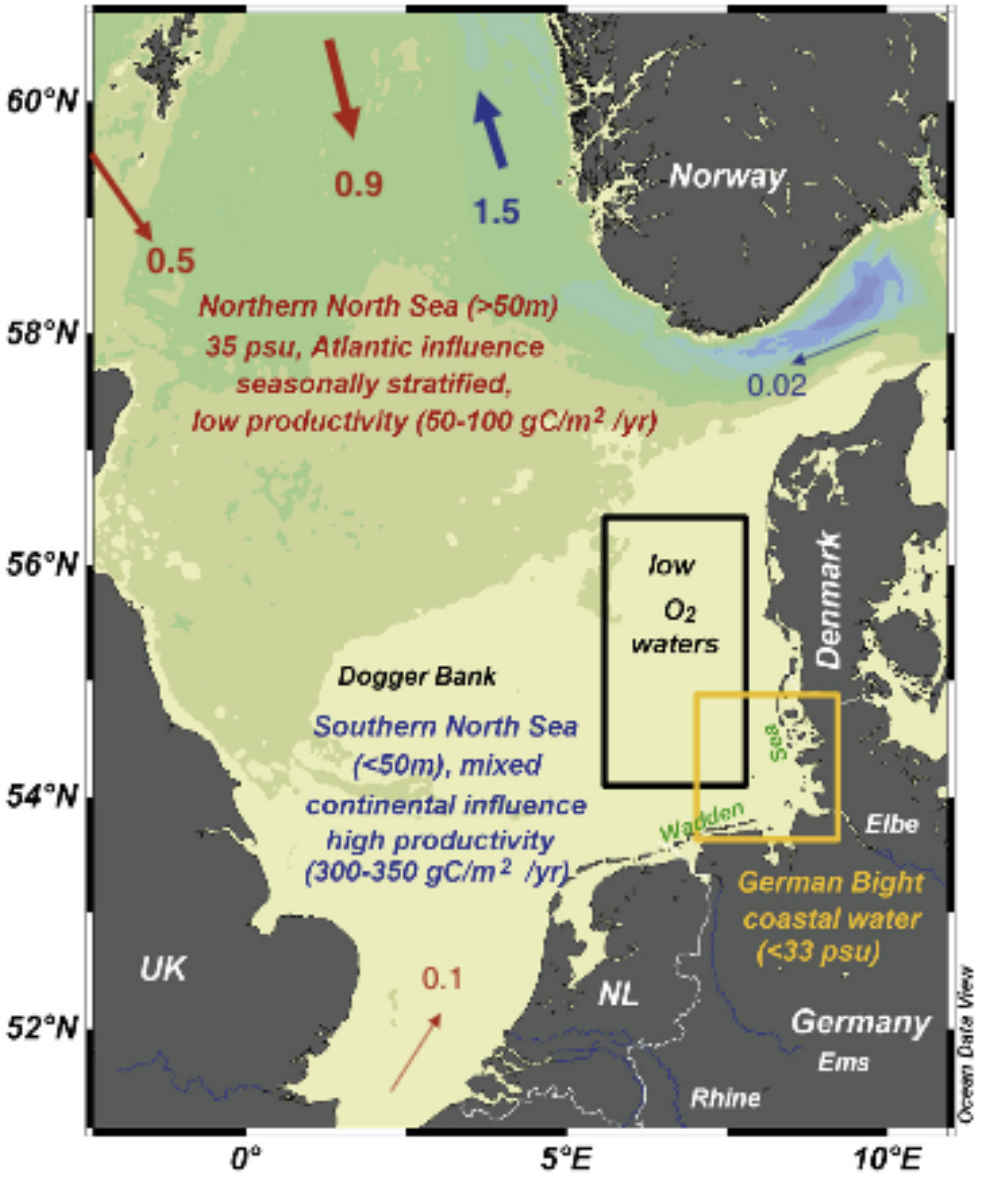

Figure 2 : map of the North sea delimited in sub-areas according to general features marked by text. Arrows with numbers denote average water mass transports (in Sv). From Emeis et al. (2015)

The Northern North Sea (NNS) is much more influenced by oceanic waters and is on average much deeper (fig. 1 & 2). The NNS has therefore a higher salinity, is seasonally stratified, and has a lower productivity (50-100 g C/m^2/year). On the contrary, the Southern North Sea (SNS) is shallower and is mixed all year round. It is more influenced by continental freshwater inputs and has a much higher productivity (Emeis et al., 2015).

The NS is one of the most intensively studied sea in the world (Emeis et al., 2015; Sündermann & Pohlmann, 2011). It has a highly developed natural wealth and is an extremely productive sea (Alvera-Azcárate et al., 2021). However, its natural resources are threatened by human activities, including oil and gas exploitation, shipping, tourism, overfishing, aggregate

extraction and dumping, and offshore wind farming (Ducrotoy & Elliott, 2008; Emeis et al., 2015; Ruddick et al., 2008). Since the early 1960s, there have been calls about the danger of nutrient pollution and eutrophication in the NS. In consequence, The NS states have agreed within the Oslo and Paris Commission for the Prevention of Marine Pollution (OSPAR) to regularly assess the eutrophication status of their waters (Claussen et al., 2009) and to take various measures to prevent the NS ecosystems from degradation. These measures mainly consist in different decrees aiming at reducing the nutrient pollution of the NS. For example, the Water Framework Directive (WFD, Directive 2000/60/EC), focuses on inland and coastal waters (Ferreira et al., 2011). The Marine Strategy Framework Directive (MSFD, Directive 2008/56/EC) on the other hand requires the European member states to achieve a Good Environmental Status (GES) of their seas by 2020 (Desmit et al., 2015, 2020; Lenhart et al., 2010; Dimitri van der Zande et al., 2019).

Since 1990, these measures have resulted in reductions in nitrate and phosphate concentrations in inland surface waters and in certain parts of the NS (Desmit et al., 2020). Despite these measures, many coastal areas of the NS still suffer from eutrophication problems such as the SNS, which affects negatively the marine environment (Gypens et al., 2009; Lancelot et al., 2005; Prins et al., 2012; van der Zande et al., 2019).

I.2. The Southern North Sea

1.2.1. Main characteristics

Ths SNS consists in a tidal mixing zone which features low water depths, strong mixing of the water column, low salinities, diminished ocean influence and high riverine nutrient inflow. These characteristics make the SNS conducive to supporting high biomass production (Xu et al., 2020). The catchment of the continental rivers discharging in the SNS covers 428 000 km^2 and is densely populated (184 millions inhabitants), highly industrialized and intensively farmed (Emeis et al., 2015). Suspended Particular Matter concentrations (SPM) are high in the shallow coastal waters of the SNS and are lower offshore. They come from different sources: the Atlantic Ocean, the Baltic sea, continental rivers, coastal erosion, the atmosphere (dust), seafloor erosion, but also from human activities such as dredging and mining operations. Nutrient concentrations have a strong seasonal cycle with a peak in December-January and a minimum during June-July

when the phytoplankton spring bloom has mobilized most of the available nutrients (Rousseau et al., 2008; Ruddick et al., 2008).

The SNS is a sensitive area suffering from various environmental problems because of high riverine pollutant inputs coming from its catchment. In addition, climate change and the associated rising of temperatures and sea level add other threats on the SNS ecosystems, which are particularly sensitive as coastal ecosystems (Desmit et al., 2020; Xu et al., 2020).

1.2.2. Eutrophication in the SNS

Coastal areas of the SNS are at high risk of eutrophication, an ecological process resulting from an increase of nutrient inputs in the ecosystem. According to the OSPAR definition, eutrophication is "the enrichment of water by nutrients causing an accelerated growth of algae and higher forms of plant life to produce an undesirable disturbance of the balance of the organisms present in the water and the water quality of the water concerned" (Lenhart et al., 2010). In other words, eutrophication is the process of enrichment of a water body with excess plant nutrients (mainly phosphorous and nitrogen), which lead to an increased primary production (Istvánovics, 2009). The eutrophication process is generally caused by human activities. However, physical factors such as geomorphology, water depth or the different currents prevailing in the system can be of great importance in the eutrophication process (Karydis & Kitsiou, 2014; Kitsiou & Karydis, 2011). Eutrophication of the SNS is mainly due to riverine inputs, either from a local source (e.g. The Scheldt) or by transboundary inputs (south-west Atlantic waters enriched by the Seine and the Somme). The influence of local or transboundary sources will depend on the human activities in the watersheds but also from large-scale climatic phenomena, such as the North Atlantic Oscillation (NAO) (Claussen et al., 2009; C Lancelot et al., 2005; Lancelot et al., 2009).

The nutrient enrichment of coastal areas can lead to the formation of large algal blooms (some of which can be toxic), an increased primary production, an increased turbidity with subsequent loss of submerged aquatic vegetation, an oxygen deficiency (hypoxia or even dead zones), changes in the community structures, or a decreased biodiversity (Banks et al., 2011; Desmit et al., 2020; Gypens et al., 2009). In the SNS, eutrophication problems are mostly visible as huge undesirable algal blooms developing during Spring. These massive spring blooms consist mainly in ungrazable colonial forms of the haptophyceae *Phaecosytis globosa*. These blooms may alter the marine food web or change the community structure (Gypens et al., 2009;

Joint & Pomroy, 1993; Lancelot et al., 2005; Lancelot et al., 1997; Lancelot et al., 2009; Passy et al., 2013; Rousseau et al., 2008; Rousseau et al., 2013).

I.2.3. Phytoplankton blooms in the SNS

Phytoplankton blooms are at the basis of the marine food web, driving biogeochemical cycles, producing oxygen and acting as a carbon pump (Xu et al., 2020). Phytoplankton spatial and temporal dynamics can be influenced by several factors, including the availability of nutrients and light, water temperature, and grazing (Capuzzo et al., 2015, 2017; Xu et al., 2020). Phytoplankton or algal blooms are generally defined as a rapid increase in the biomass of algae in an aquatic system (van der Zande et al., 2012). In the SNS, the phytoplankton bloom succession consists in a first moderate diatom bloom in late February-early March. This moderate bloom is rapidly followed by a huge biomass peak of *Phaeocystis globosa* occuring in late April-early May, just before summer (Gypens et al., 2009; Gypens et al., 2007;Lancelot et al., 2005; Leynaert et al., 2002; V. Rousseau et al., 2008). This bloom is often referred as being the spring bloom and constitutes the majority of the annual primary production. The autumn can also show a small diatom bloom (Muylaert et al., 2006; Anja Nohe et al., 2020; Philippart et al., 2009; Speeckaert et al., 2018). The *phaeocystis* bloom is fueled by freshwater riverine inputs enriched in nitrogen (N) and phosphorus (P), but deficient in silicon (Si, required by diatoms) (Lancelot et al., 2005; Passy et al., 2013; Rousseau et al., 2013; Speeckaert et al., 2018).

Phaeocystis spring blooms were already reported in the late 1890s and can be therefore considered as a natural phenomenon. However, these blooms tend to be more intense and last longer (the duration and cell numbers in these blooms increased at least fivefold over the 1970s -1980s period due to the intense eutrophication of the SNS) (Desmit et al., 2015). Although *Phaeocystis* is not considered as an harmful algae bloom (HAB) specie, high cell abundances may result in the formation of large colonies that are inedible to many zooplanktons species. Intense *Phaecosystis* bloom in the SNS thus constitute a potential decrease in zooplankton grazing and a significant loss for higher trophic levels (Desmit et al., 2015; Lancelot et al., 2005; Lancelot et al., 2009). Furthermore, intense *Phaecocystis* colonies can cause the clogging of fishing nets, which reduces the amount of catch and causes commercial losses (Weisse et al., 1994). Finally, when *Phaecosytis* blooms decay, it often results in the beaching of odorous white foam (fig. 3) on the coast which can cause health problems in the worst cases (Lancelot et al., 2005; van der Zande et al., 2019; van der Zande et al., 2012). Figure 3 shows the massive beaching of marine foam caused by intense blooms of *Phaeocystis*.

Figure 3 : Bleaching of sea foam on a Dutch beach. Source : https://www.seos-project.eu/oceancolour/oceancolour-c03-p05.html/

Phaecosytis blooms can thus be considered as an ecological nuisance and high spring chlorophyll concentrations indicate an undesirable status of the SNS.

I. 3. Satellite data as a monitoring tool for eutrophication

The OSPAR strategy aims to eliminate eutrophication in the SNS (MSFD) (Lenhart et al., 2010). To achieve this goal, it is important to make a robust statement of the situation by monitoring all aspects necessary to assess the eutrophication status of a given area (Lenhart et al., 2010). Any long-term change and/or variability of the SNS eutrophication state require analysis of consistent and homogeneous data. There are different sources and types of data, all of which have their own advantages and disadvantages (Emeis et al., 2015; Karydis & Kitsiou, 2014; Kitsiou & Karydis, 2011). In-situ observations are usually considered as relatively robust and reliable data and are still used as the main monitoring tool to assess the environmental status of the SNS (van der Zande et al., 2019). However, the European Commission has pointed out the lack of consistency in the in-situ monitoring approaches made by each country bordering the NS. In addition, in-situ sampling campaigns are expensive, time and personnel-consuming and

in-situ measurements only give us very limited information in time and space (Emeis et al., 2015; van der Zande et al., 2019)

During the last decades, with advances in space science, computing applications and increased computer powers, there has been a growing tendency to use satellite remote sensing as a supporting tool to monitoring requirements (Gholizadeh et al., 2016; Kitsiou & Karydis, 2011; van der Zande et al., 2019). Indeed, satellite remote sensing methods offer many advantages, as they are a coherent method of data acquisition and provide information with generally much greater spatial and temporal coverage than in-situ data (Banks et al., 2011; Kitsiou & Karydis, 2011; Matthews & Bernard, 2015). Satellite data are also often publicly and freely accessible. The monitoring requirements needed by the OSPAR convention can be considerable due to the extensive coastline of the SNS (Ruddick et al., 2008). In addition, satellite data allow to overcome the differences in methodology used by the different states, which allows to perform a more consistent assessment of the SNS eutrophication status. Hence, the use of satellite data offers a powerful supporting tool in the assessment of large-scale eutrophication of the SNS over a long period of time (van der Zande et al., 2019)

I.3.1. Ocean color remote sensing

Different sensors mounted on satellites measure the water radiance at different wavelengths and the retained data can be used to retrieve directly or indirectly water quality parameters including CHL, SPM, turbidity, salinity, secchi disk depth, sea surface temperature (SST), sea level, or dissolved organic carbon (Gholizadeh et al., 2016; Ruddick et al., 2008). Some of the variables of interest when assessing eutrophication (CHL, SPM) can be retrieved from radiance measured by ocean color sensors operating in the visible spectrum after using different algorithms (Gholizadeh et al., 2016; van der Zande et al., 2019).

Figure 4 shows how the ocean color data acquisition works (Allan, 2008) :

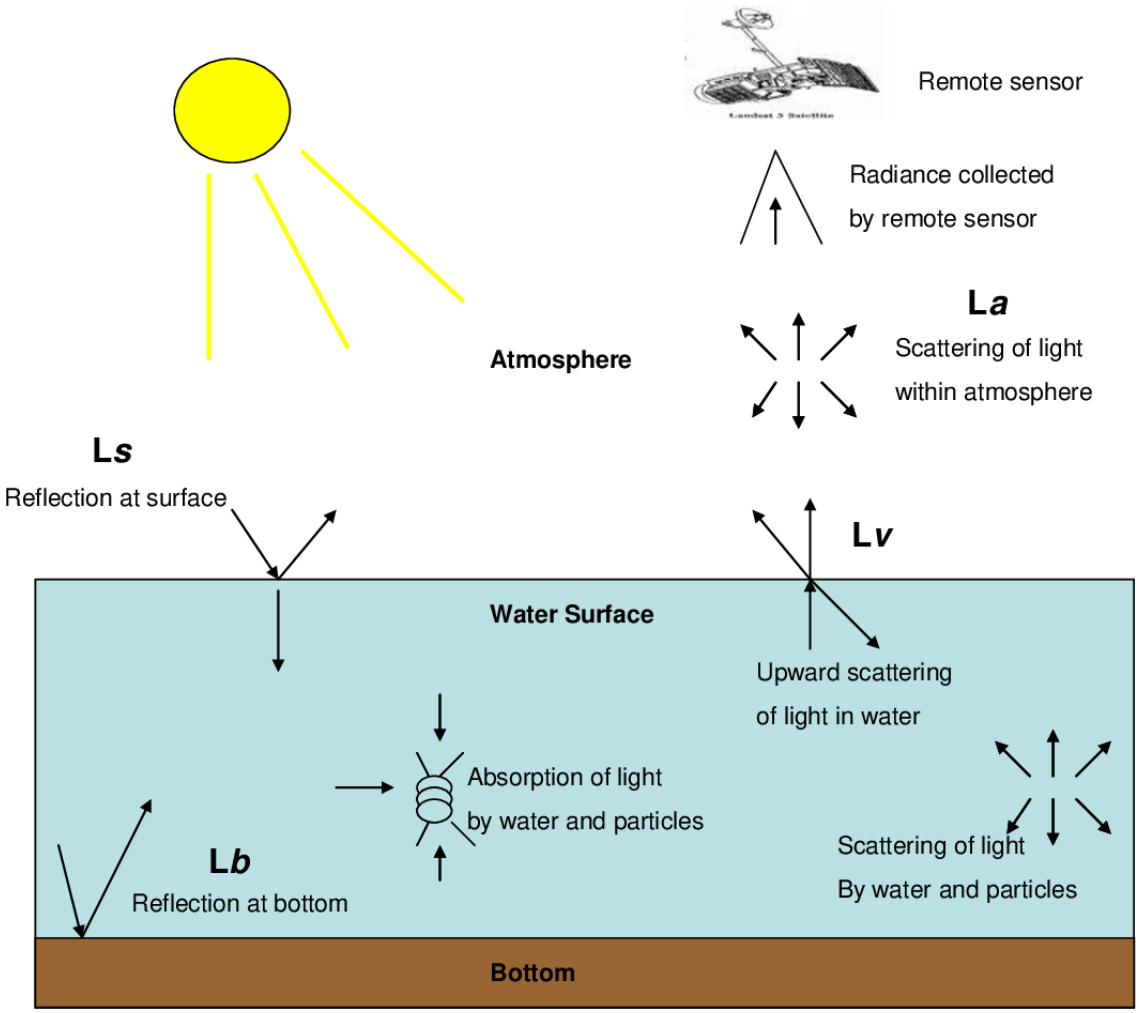

Figure 4 : schematic representation of the radiance signal received by a satellite remote sensor. Source : Allan (2008).

The radiance (L) recorded by a satellite sensor includes the following components (fig. 4) (Allan, 2008):

- La: solar and sky radiation that does not contact the air-water interface, which represents contribution from the atmosphere. Gases and aerosols in the atmosphere scatter and absorb radiation.

- Ls: reflection from the water surface, often seen as sun glints where the data is deteriorated and unusable.

- Lv: sky and solar radiation penetrating the water interface is changed by the absorbing and scattering components of the water and re-emerges from the water without contacting the sea bottom.

- Lb: sky and solar radiation that penetrates the air water-interface, reaches the sea bottom, and re-emerges from the water column.

An optical sensor looking downward measure the total radiance L = La + Ls + Lv + Lb. Only the water leaving radiance (Lv + Lb) contains information about the water constituents and bottom conditions (Allan, 2008). The atmospheric correction consists in removing the atmospheric and surface glint contributions to the radiance L to obtain the water-leaving radiance (Lv + Lb). Once the atmospheric correction is done, different algorithms allow to retrieve the concentrations of the optically active constituents of interest from the water-leaving radiance. Final products often integrate data from different satellites as well as data from in-situ measurements or from numerical modeling in order to obtain the most complete information possible.

I.3.2. Case 1 vs. case 2 waters

In deep open waters, phytoplankton is the main optically active constituent which causes variability of water colour, which goes from deep blue to green as chlorophyll-a and related pigments concentrations increase (Ruddick et al., 2008). This type of waters is commonly called “case 1” waters and retrieval algorithms such as OC4 and OC5 have been largely successful in retrieving accurate CHL for their monitoring (van der Zande et al., 2019). The SNS, which is a coastal area, is optically much more complex than case 1 waters. The variability of its color is also caused by coloured dissolved organic matter (often referred as yellow substances, coming essentially from the degradation of terrestrial vegetation reaching the sea through rivers) as well non-algal SPM (Ruddick et al., 2008). Such waters are called “case 2 waters” and retrieval of bio-geochemical parameters from ocean color data is more challenging and the algorithms used are often more complex (red-edge algorithms or artificial network approaches). Fig. 5 shows the classification diagram of case 1 or case 2 waters according to the dominance of their optical constituents.

Figure 5 : Classification diagram of case 1 and case 2 waters. Source : IOCCG (2000).

I.3.3. Limitations of remote sensing

Although the advantages of using satellite data are numerous, satellite remote sensing techniques are not infallible and still have some limitations. These limitations include (Gholizadeh et al., 2016) :

- clouds can cause many unpredictable gaps in the data, which is especially the case in cloudy regions like the SNS
- only the first meter of the water column can be monitored
- only a few parameters can be detected by remote sensing and in-situ measurements of many pollutants (such as nutrients) still need to be performed
- data quality can sometimes be problematic, especially in optically complex coastal regions where spatial resolution may pose few limitations.

These limitations mean that the use of satellite remote sensing must be done in conjunction with other methods, such as in-situ measurements (for validation and calibration) or numerical techniques (modeling, interpolating method).

I.4. Aims of the study

This master thesis mainly aims to assess long-term changes in the eutrophication status and the phytoplankton dynamics of the SNS using satellite data covering a 20 years-long period (1998 - 2017). For this purpose, spatial and temporal dynamics of CHL (a proxy for phytoplankton biomass) in the SNS will be investigated using a reconstructed satellite product (containing no gaps due to clouds). Other abiotic variables known to have an influence on phytoplankton dynamics in the SNS such as SPM, SST, precipitations (PPT) and NAO, will be analyzed. At the end, this study will allow to:

1. Assess the evolution of the eutrophication status of the SNS during the study period (1998-2017) by investigating CHL spatial and temporal dynamics. Special attention will be given to the spring blooms dynamics.
2. Identify the main factors responsible for seasonal or long-term changes in CHL dynamics in the SNS.
3. Evaluate the relevance of the use of satellite products in the long-term assessment of eutrophication in a complex coastal sea such as the SNS.

CHAPTER II : MATERIAL AND METHODS

II.1. Domain of the study

The study domain is shown in figure 6 (red rectangle) and consists of the SNS and the easternmost part of the English Channel. This part was also added to the domain because it is strongly interacting with SNS. The coordinates of the domain go from 48°N to 53.5°N and from 3.5°W to 9.5°E. The total domain constitutes an area of approximatively 550 000 km^2.

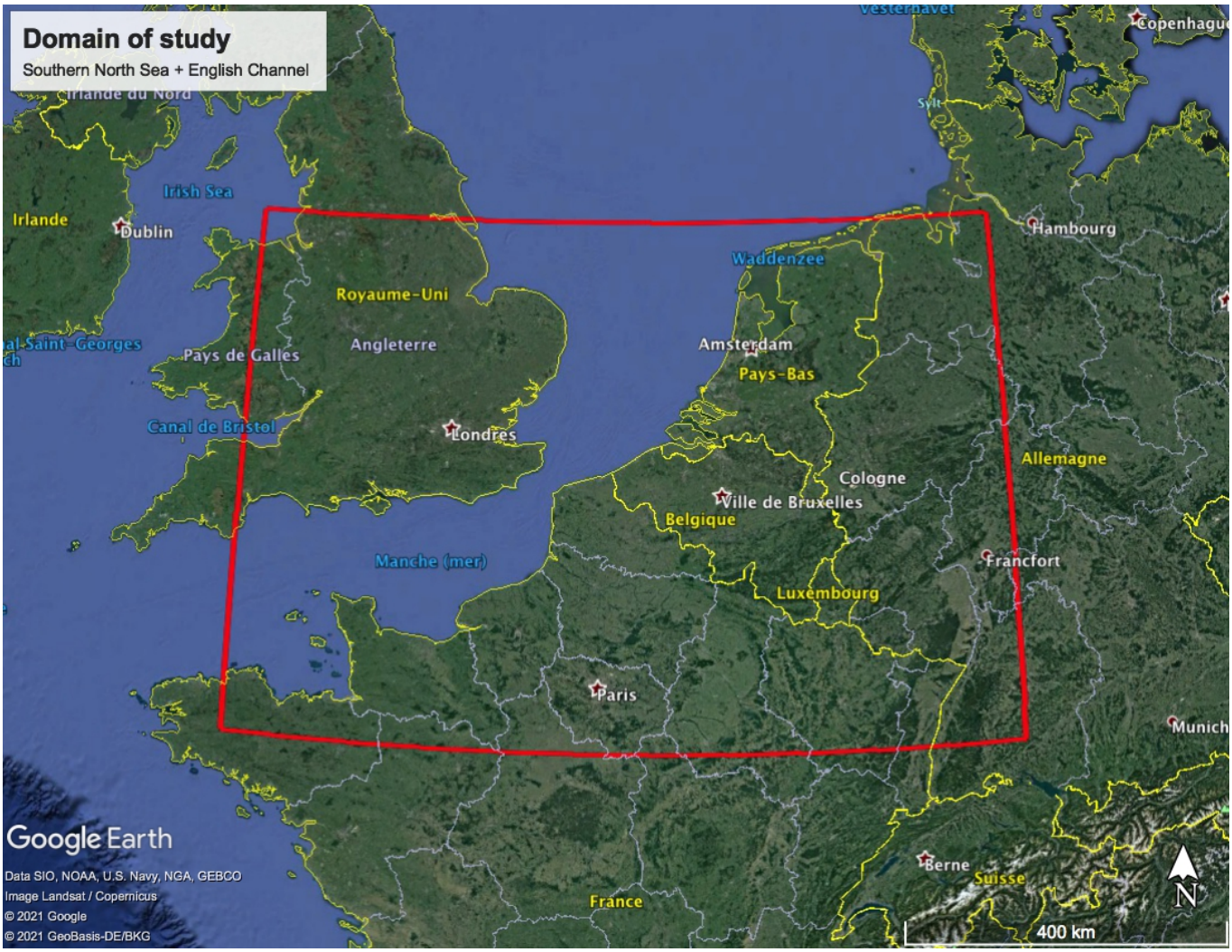

Figure 6 : domain of study (red rectangle). This map comes from Google Earth application.

II.2. Data

Table 1 summarizes the different products used for the study. Details of each product can be found in dedicated sub-sections.

Product	Type of data	Spat. res.	Temp. res.	Source	Remark
Chlorophyll (CHL)	Reconstructed multi-satellite product (level 4)	~ 1 km	Daily	GHER + RBINS	November – mid-February data are missing
Suspended Particular Matter (SPM)	Reconstructed multi-satellite product (level 4)	~ 1 km	Daily	GHER + RBINS	December – mid-February data are missing
Sea Surface Temperature (SST)	Reprocessed multi-satellite product (level 4)	0.05° x 0.05° (lat x long)	Daily	CMEMS	product identifier: SST_ATL_SST_L4_REP_OBSERVATIONS_010_026
Precipitations (PPT)	Merged in-situ observations + satellite + forecast data	2.5° x 2.5° (lat x long)	Monthly mean	NOAA PSL	Enhanced version of CMAP using forecast data
North Atlantic Oscillation (NAO)	Observations + EOF analysis data	/	Monthly mean	NOAA NCDC	/

Table 1 : Summary presenting the type, the spatial, temporal resolutions and the source of the different data products used. Details of each product can be found in the following dedicated sub-sections.

II.2.1. Chlorophyll

The CHL product used in this study is a reconstructed (level 4, containing no gaps) multi-satellite product containing daily 1-km spatial resolution CHL data. CHL data are expressed in mg Chl.m^{-3} (= µg Chl/L). The product covers a period from 1998 to 2017. This product comes from the GeoHydrodynamics & Environment Research laboratory (GHER, ULiège) and was generated using the DINEOF method (Data Interpolating Empirical Orthogonal Functions, (Alvera-Azcárate et al., 2005; Beckers & Rixen, 2003) over the SNS domain. DINEOF is a technique to reconstruct missing data in geophysical datasets. This method is based on the decomposition of an initial dataset into its empirical orthogonal functions, to interpolate missing data. This method is particularly well suited to reconstruct satellite datasets in the NS for which many data may be missing due to clouds (which impede the electromagnetic radiation to reach the satellite sensors). Because of the poor quality of the initial data during November – mid–February (due to the strong cloud coverage which creates many gaps), these months have been excluded from the DINEOF analysis. Therefore, only data from mid-February to late October were used in the study for each year. More details on the DINEOF technique can be found in Beckers and Rixen (2003), Alvera-Azcárate et al. (2005), Alvera-Azcárate et al. (2009) or on this website : http://modb.oce.ulg.ac.be/mediawiki/index.php/DINEOF.

The initial dataset reconstructed by DINEOF is a level-3 product (containing gaps due to clouds) coming from the Royal Belgian Institue of Natural Sciences (RBINS). This product was generated using the JMP-EUNOSAT approach (van der Zande et al., 2019) using publicly accessible data available from the Copernicus Marine Environment Monitoring Services (CMEMS), European Space Agency and other data providers (i.e. IFREMER). This approach consists in using a mix between different quality controlled CHL algorithms (OC5 and Gons algorithms) depending on the type of water encountered (clear waters of case 1 or turbid waters of case 2) (van der Zande et al., 2019; Alvera-Azcárate et al., 2021). More details can be found in van der Zande et al. (2019) and Lavigne et al. (2021)

II.2.2. Suspended particulate matter

The SPM product used in this study also consists in a multi-satellite product of level 4 containing daily 1-km spatial resolution SPM data reconstructed by the DINEOF method (GHER, ULiège). The SPM product covers a period going from 1998 to 2021 (with year 2019 missing) and SPM are expressed in mg/L. As for the CHL product, bad winter data (here, December – mid-Ferburary) were excluded from the DINEOF analysis.

The initial SPM level-3 product was given by the RBINS. SPM data were generated by applying the generic turbidity algorithm used in Nechad et al., (2010) to the OC-CCI Remote Sensing Reflectances (at 665 nm) obtained from the CMEMS data portal (product identifier: OCEANCOLOUR_ATL_OPTICS_L3_REP_OBSERVATIONS_009_066).

II.2.3. Sea surface temperature

SST product used in this study is a level-4 reprocessed satellite product containing daily gap-free SST at 20 cm depth (in °K). It has been downloaded from the CMEMS data portal (product identifier: SST_ATL_SST_L4_REP_OBSERVATIONS_010_026). This product uses multi-satellite data coming from the European Space Agency Sea Surface Temperature Climate Change Initiative (ESA SST CCI) level-3 product (1982 - 2016) and from the Copernicus Climate Change Service (C3S) level-3 product (2016 - 2019) to generate gap-free SST data of 0.05° x 0.05° (lat x long) spatial resolution from 1982 to 2019.

II.2.4. Precipitations

PPT data come from the CPC Merged Analysis of Precipitation product (CMAP) and have been downloaded from the National Oceanic and Atmospheric Administration Physical Sciences Laboratory data portal (NOAA PSL, https://psl.noaa.gov/data/gridded/data.cmap.html#detail). CMAP is a technique which produces pentad or monthly analyses of PPT (in mm/day) in which PPT measures from rain gauges are merged with satellite-derived PPT estimates (infrared and microwave sensors) (Arkin et al. 2020). The data have a 2.5° x 2.5° spatial resolution grid and goes from 1979 to present. In this study, we used an "enhanced" version of the product (CMAP/A), which fill the data gaps with PPT forecasts from the National Centers for Environmental Prediction (NCEP) and the National Center for Atmospheric Research (NCAR) reanalysis. For our purpose, we used the monthly estimates over the 1998 - 2017 period.

II.2.5. North Atlantic Oscillation

The North Atlantic Oscillation index (NAO) is an index based on the sea-surface pressure difference between the Subtropical (Azores) High and the Subpolar Low pressures (Rousseau et al., 2008). The NAO influences greatly the meteorological and hydrological conditions in the SNS. Monthly NAO index data were obtained from the NOAA National Climatic Data Center portal (NOAA NCDC, https://www.ncdc.noaa.gov/teleconnections/nao/). These monthly NAO index data are available since 1950 and have been obtained from the procedure described in Barnston & Livezey, (1987). It is calculated by projecting the NAO loading pattern to the daily anomaly 500 millibar height field over 0-90°N. The NAO loading pattern has been chosen as the first mode of a rotated empirical orthogonal function analysis using monthly mean 500 millibar height anomaly data from 1950 to 2000 over 0-90°N latitude. More details on the method can be found here : https://www.cpc.ncep.noaa.gov/products/precip/CWlink/daily_ao_index/history/method.shtml

II.3. Data analysis

II.3.1. R and RStudio

All the data were analyzed using R scripts that were written through its dedicated RStudio integrated development environment. R is a programming language designed mainly for statistical and graphics computing. It is supported by the R Foundation for Statistical Computing. The R language is largely used by statisticians, data miners and data scientists for statistical computing and data analysis. The strength of R lies in the large number of existing packages. Indeed, the R community is strongly involved in the development of the software and more than 16 000 packages have been developed. This large number of existing packages also explains why many geostatisticians use R.

II.3.2. Chlorophyll

A. Spatial variability

Spatial variability of CHL was first assessed by mapping the temporal averaged CHL over the 1998 – 2017 period. To avoid that extreme values localized in very specific locations (e.g. Ijsselmeer and Markermeer, Netherlands, which are not part of the SNS) impact the contrast of

the color bar, a CHL mean limit of 10 µg Chl/L has been introduced. Secondly, the spatial variability of CHL was also investigated over time by mapping the monthly-averaged CHL for each month (March to October, February being excluded because the month is incomplete). These monthly climatologies are calculated from the monthly CHL means during the 1998 – 2017 period. Here, a limit of 15 µg Chl/L was applied for all months for the same reasons as described above.

B. Temporal variability

Temporal variability of CHL was assessed by computing daily time series of domain-averaged CHL during the study period. In order to eliminate daily variability and smooth the data, a Gaussian low-pass filter with a 30-day window was applied. These time series allow us to study the seasonal CHL variability, as well as the interannual variability. In addition, the main statistics (yearly mean, yearly maximum and its timing) were also calculated for each year in order to facilitate interannual comparison of CHL data. Temporal trends of CHL were assessed using a simple linear fit model of the main CHL statistics to the years over the study period (1998 – 2017).

C. Spring Bloom determination and onset

Phytoplankton spring bloom phenology is of particular importance in a marine ecosystem because its matching with zooplankton cycles may affect the rest of the trophic chain. The spring phytoplankton bloom can be monitored through the remotely sensed ocean color CHL peak observed during spring in the SNS (Brody et al., 2013). Various methods exist to determine the spring bloom onset and offset from CHL. In this work, we used one of the methods reviewed by Brody et al. (2013) which consists in determining a threshold value which is calculated as follows (eq. 1):

$$Threshold_{CHL} = M_{CHL} + M_{CHL}.5\ \% \quad (1)$$

Where $Threshold_{CHL}$ is the threshold value and M_{CHL} is the yearly median of CHL data. The first day when domain-averaged CHL exceeds $Threshold_{CHL}$ is defined as the spring bloom onset ($onset$). The day when the domain-averaged CHL falls below $Threshold_{CHL}$ is defined as the bloom offset ($offset$) . This method also allows us to calculate the total duration (in days) of the spring bloom as follows (eq. 2) :

$$bloom\ duration = offset - onset \quad (2)$$

Once the spring bloom window was determined, we were able to calculate the spring bloom mean for each year (CHL bloom mean). The timing of the maximum CHL (i.e. the date when CHL attains its maximum value) was also analyzed.

II.3.3. Suspended particulate matter

In order to assess the temporal variability of SPM, time series of the daily domain-averaged SPM were performed over the 1998-2021 period (with year 2019 missing). As for CHL, data were smoothed using a 30-day window Gaussian filter. Principal statistics (mean, median, winter maximum and summer minimum) were also computed to facilitate interannual comparison and temporal trends. In addition, we made a sub-set to retain only the wintertime data (February – end of March). The temporal trends were assessed by using a simple linear fit model of the main statistics to the years, going from year 1998 to year 2017 (last year of available CHL data).

II.3.4. Sea surface temperature

The SST data were first converted from °K to °C. In order to visualize the temporal variability of the temperature (seasonality + interannual variability), time series of the daily domain-averaged SST were computed over the 1998-2019 period. To visualize the trend of SST over the 20-years study period, we must get rid of the seasonality signal. This was done by computing the moving mean with a 365-day window.

For each year, main statistics (yearly mean, yearly maximum) were calculated. We also calculated the wintertime mean (i.e. January – mid-April mean) as SST of this period are expected to have the most impact on the spring bloom phenology. The temporal trends were assessed by using a simple linear fit model of the main statistics (rolling mean, yearly and wintertime means, yearly maximum) to the years (1998-2017).

II.3.5. Precipitations

Since the temporal and spatial resolution of the PPT product is much lower (monthly averages, for a spatial resolution of 2.5° x 2.5°), we proceeded differently. For each year, we first calculated the yearly domain-averaged PPT to investigate the 20-year period trend of the global PPT over our domain. We also calculated the wintertime domain-averaged PPT mean (January - April). This allows us to look more precisely at the trend of winter PPT, which are expected to have the most impact on the spring bloom dynamics.

II.3.6. North Atlantic Oscillation

It is during the winter that the NAO shows the most variability and is the most determinant regarding the meteorological and hydrological conditions in the SNS (Rousseau et al., 2008; Thomas et al., 2018). For this reason, we have calculated the wintertime mean (January - April) of the NAO index for each year over the 1998-2017 period.

II.3.7. Correlation analysis

To determine which variables are correlated with each other (positively or negatively), a correlation matrix between all relevant variables was performed. Table 2 show us all the relevant variables chosen for the analysis. Related variables (such as CHL maximum and CHL bloom mean, or SPM winter maximum and SPM wintertime mean) were reduced to one variable in order to avoid redundancy and to make the graph more readable. For all abiotic variables (SPM, SST, PPT and NAO), the annual mean as well as the wintertime mean have been chosen, as we expect that environmental conditions during this season have a greater influence on spring bloom dynamics (Thomas et al., 2018). Moreover, the variable "year" has been removed because the temporal trend over the period of each variable is already discussed in their corresponding results section.

Variable name	Variable explanation	Units
onset	Onset date of the spring bloom in the year	Date in the year (mm-dd)
duration	Spring bloom duration	Days
CHL_total	CHL yearly mean	µg Chl/L
CHL_bloom	CHL mean during the spring bloom	µg Chl/L
SPM_total	SPM yearly mean	mg/L
SPM_winter	SPM mean during winter	mg/L
SST_year	SST yearly mean	°C
SST_winter	SST mean during winter	°C
PPT_year	PPT yearly mean	mm/day
PPT_winter	PPT mean during winter	mm/day
NAO_winter	NAO mean during winter	No unit (index)

Table 2: Variables chosen for the correlation analysis and their explanation. Redundant variables and time were excluded from the correlation analysis.

For the analysis, we used the Pearson's coefficients (*r*). Consider a variable X and a variable Y. The Pearson's coefficient is a measure of linear correlation between variables X and Y and is defined as follows:

$$r = \frac{\sum_{i=1}^{n}(X_i - \bar{X})(Y_i - \bar{Y})}{\sqrt{\sum_{i=1}^{n}(X_i - \bar{X})^2}\sqrt{\sum_{i=1}^{n}(Y_i - \bar{Y})^2}} \quad (3)$$

Where X_i $(\text{or } Y_i)$ = value of the variable X (or Y) for year i and $\bar{X}$ $(\text{or } \bar{Y})$ = mean of the variable X (or Y). Pearson's coefficient is thus a measure of the normalized covariance, such that the result always has a value between −1 (perfect negative correlation) and 1 (perfect positive correlation). A value of 0 reflects a null relationship between the two variables. The *p-value* of each Pearson coefficients was then calculated.

CHAPTER III : RESULTS

III.1. Chlorophyll

III.1.1. Spatial variability

Figure 7 presents the spatial distribution of the temporal CHL mean in the SNS calculated over the entire study period (1998-2017). Figure 8 shows the monthly CHL climatologies (March – October).

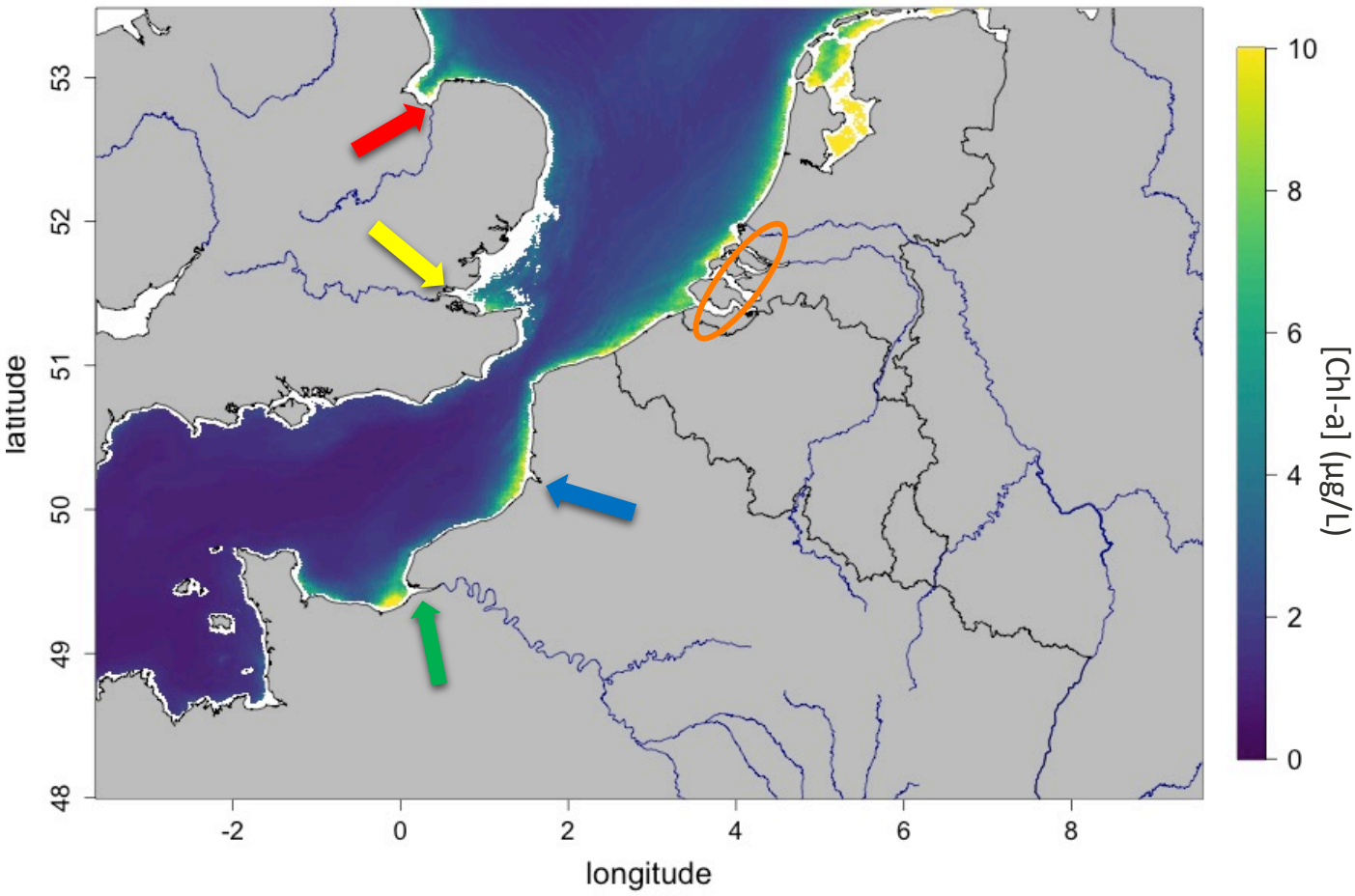

Figure 7 : Spatial distribution of the temporal (1998-2017) CHL mean in the SNS. Yellow arrow: the Thames mouth ; red arrow : the Great Ouse mouth ; green arrow : the Seine mouth ; blue arrow : the Somme mouth ; orange ellipse : the Rhine – Meuse - Scheldt delta.

Highest CHL means (~10 µg Chl/L) in the SNS are mainly distributed along the Belgian, the Dutch and the northern France coastal zone (fig. 7). The coastal area of eastern England also shows CHL-rich waters, although these concentrations appear to be more moderate. CHL are also generally higher at the mouths of large rivers such as the Thames (yellow arrow, even if data are missing because of the low number of observations), the Great Ouse (red arrow), the Seine (green arrow), the Rhine – Meuse – Scheldt (orange ellipse) or even the Somme (blue arrow). High CHL means are also found in the Wadden Sea, along the northern coasts of the Netherlands. A gradient of CHL can be generally seen from the coasts (higher CHL) to open waters (lower CHL), with open waters being much less rich in CHL (~3-4 µg Chl/L). The open waters of the English Channel are particularly low in CHL (~ 2 µg Chl/L).

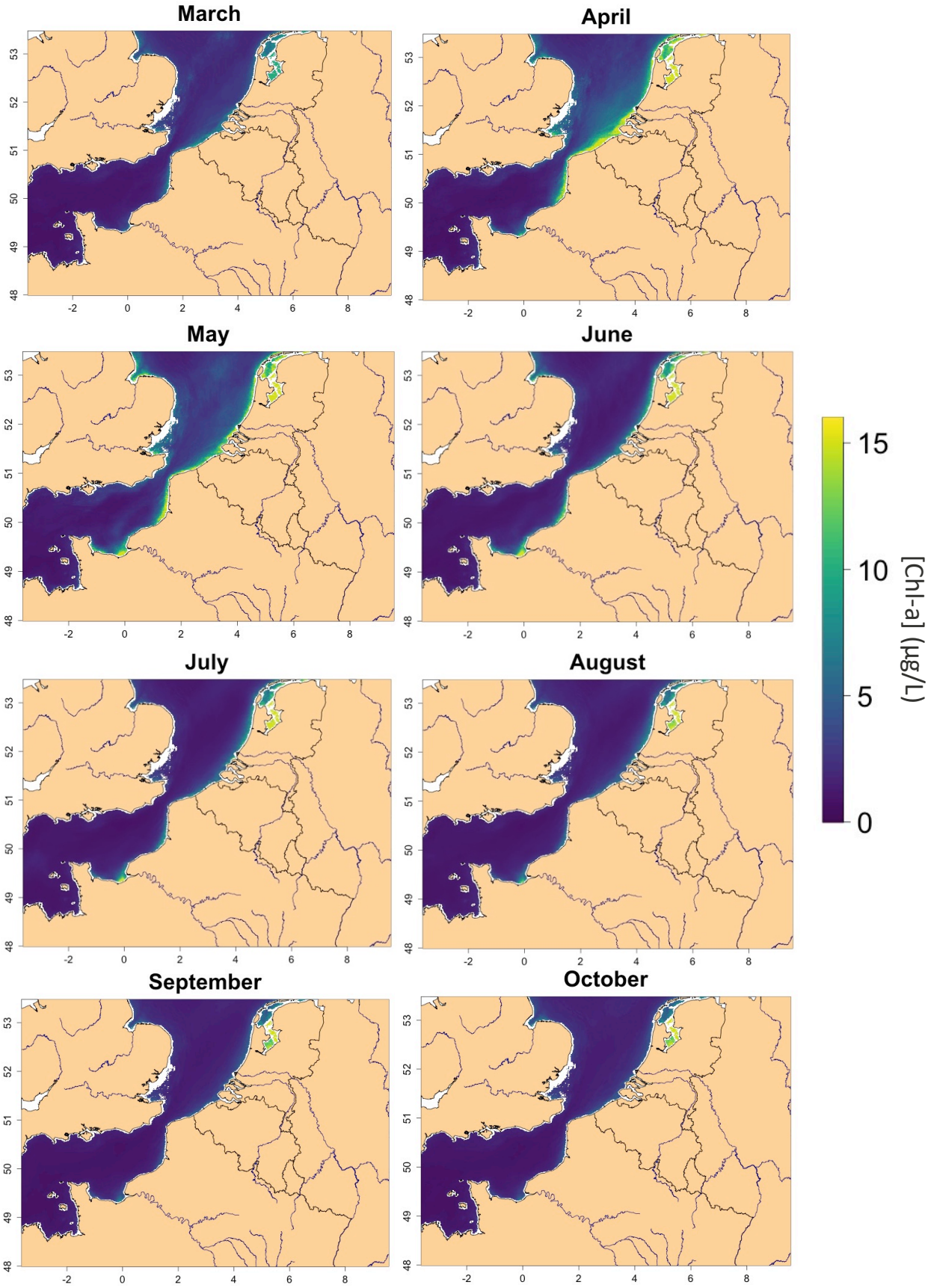

Figure 8 : Monthly climatologies of CHL (March – October) in the SNS. These spatial distributions have been obtained from the monthly data of each year between 1998-2017. Only months for which data were complete (March - October) are presented.

Fig. 8 informs us not only about the spatial distribution of the mean CHL according to months, but also about the overall seasonality patterns. We can identify that during March (fig. 8), CHL start to get already relatively high especially along the coast. April corresponds to the blooming month (mainly in the coastal zone), where very high CHL means (~ 15 µg Chl/L) are observed and are the most widespread. Although these high CHL means are mostly distributed along the coast (French, Belgian and Dutch coastal zones essentially), moderate - high CHL means (~10 µg Chl/L) are also observed further offshore, especially in the lower latitudes of the southern bight of the SNS. During May, CHL means remain very high, especially along the coastlines. High CHL means also appear in the open waters of the highest latitudes of the domain, meaning that the timing of the spring blooms in these waters may be delayed in comparison to the coastal areas. During June, moderate – high CHL means are almost exclusively located along the coasts and the river mouths. During July and August, concentrations are lower but still moderate – high CHL means can still be found along the coasts and the main river mouths. This indicates that summer – late summer blooms can be observed along the coastal zone. September and October show low CHL means (<1.5 µg Chl/L) in most part of the domain. Coastal regions can still exhibit moderate CHL means (~4-5 µg Chl/L in certain area such as the Seine river mouth).

III.1.1. Temporal variability

A. CHL seasonality

Figure 9 represents the typical seasonal variation of the domain-averaged CHL mean in the SNS. Here, year 2011 has been chosen as an example.

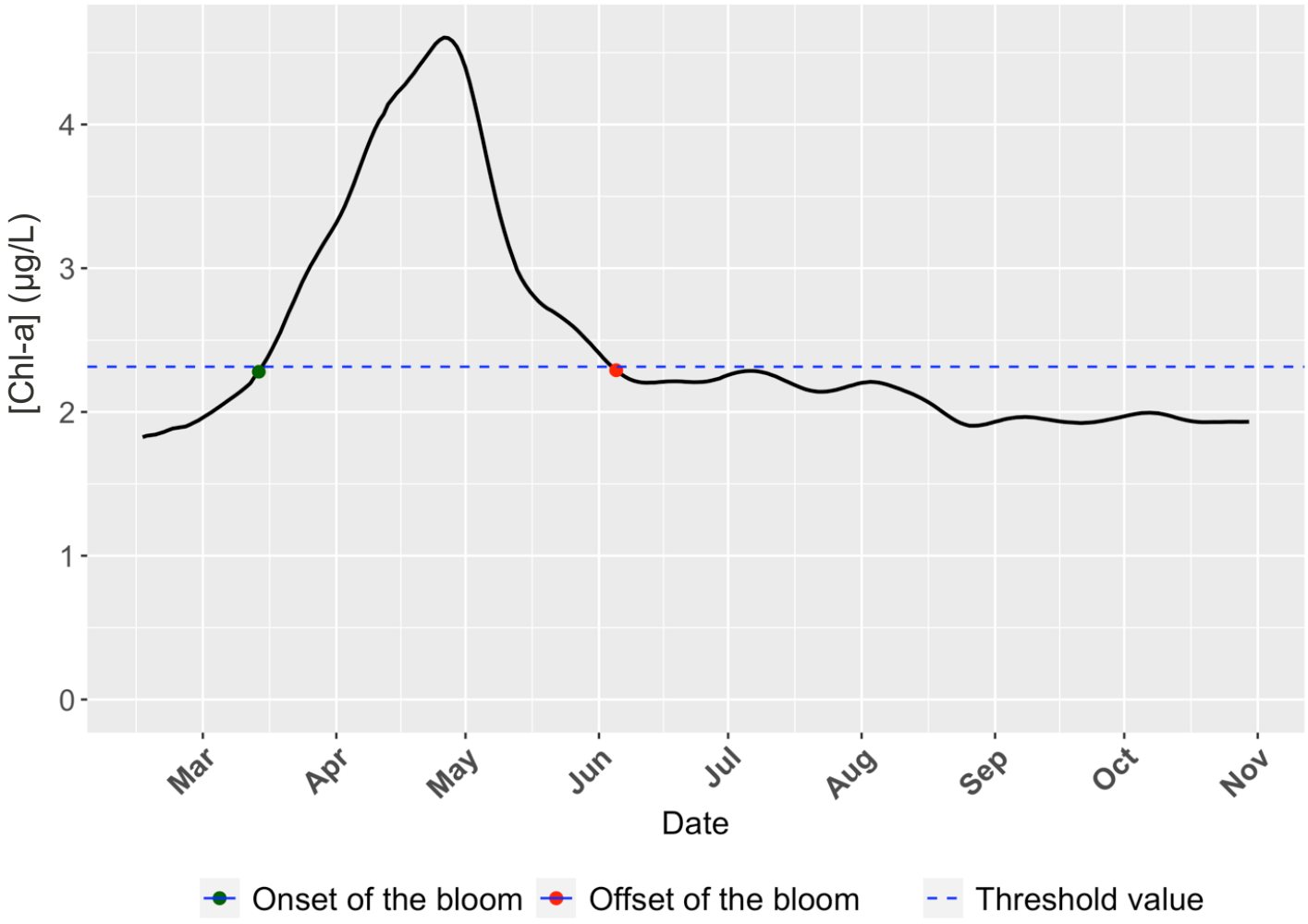

Figure 9 : Typical seasonality of the domain-averaged CHL in the SNS (year 2011). The spring bloom is delimited by an onset and an offset date, which are determined by a threshold value calculated with equation (1) in section II.3.2.C.

Domain-averaged CHL of year 2011 show a typical curve reflecting the strong spring bloom dynamic occurring in the SNS domain. CHL start to increase rapidly around the beginning of March and the spring bloom onsets around mid-March once CHL reach the threshold value for the first time (green point, as defined in section 2.3.2.C). CHL continue to increase (climax phase) to reach its maximum around end-April (apex of the bloom, with CHL ~4.6 µg Chl/L) (Llort et al.,

2015). After its apex, the bloom starts to decrease rapidly (decline phase). The spring bloom offsets when CHL pass below the threshold value (red point), about 1 month after having reached its maximum. After the spring bloom, we observe two flattened summer – late summer CHL signals, after what CHL decrease at the beginning of fall and remain relatively stable through the rest of the year.

B. CHL interannual variability

Figure 10 shows the time series of the domain-averaged CHL (fig. 10.A) as well as the key statistics of CHL (CHL maximum, yearly and spring bloom CHL means) for each year (fig. 10.B).

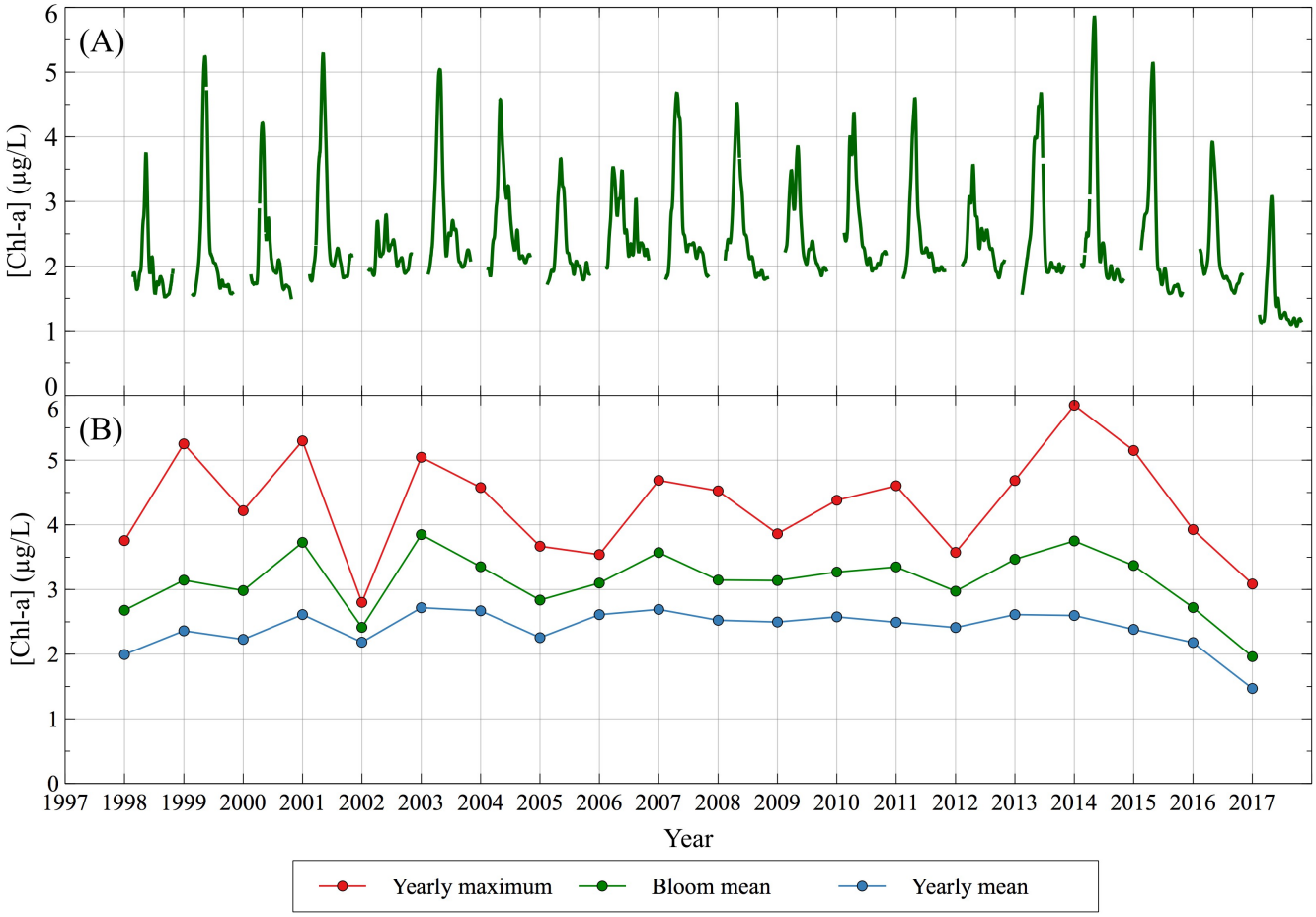

Figure 10 : Temporal variability of CHL during the study period (1998 – 2017), in µg Chl/L. (A) : domain-averaged CHL time series. November – mid-February data are missing due to the intense cloud coverage during these months ; (B) : CHL main statistics (yearly maximum, spring bloom and yearly means) according to the year.

Note that November – mid-February data are missing so the yearly mean can be slightly overestimated. We can observe in the CHL time series (fig. 10.A) that the spring bloom dynamic

described in the previous section (III.1.1.A) is almost present for every year (except year 2002, which show an atypical signal). Some years show also a late summer bloom signal (year 2003, 2006, 2009 and 2012) (fig. 10.A). Regarding the CHL maximum, we observe a strong interannual variability, with some years having particularly low (year 2002 or 2017) or high (year 2001, 2003 or 2014) CHL peak. Highest CHL of the time series are obtained in the CHL peak of 2014, in spring (5.9 µg Chl/L), whereas lowest CHL is obtained in fall 2017 (1.2 µg Chl/L). Logically, the bloom means (fig. 10.B) are well correlated with CHL peaks (fig. 10.A), indicating that high CHL peak years show overall intense spring blooms.

When looking at the CHL yearly mean (fig. 10. B), CHL appear to increase from 1998 (2 µg Chl/L) to 2003 (2.65 µg Chl/L). Then, except for the year 2005 (which shows lower CHL), CHL yearly means seem to be relatively stable until 2014, from where CHL yearly mean start to decrease until the end of the study period. Regarding trends over the period (linear fit), no trend of increase or decrease was noticed for all main statistics (p-value >> 0.05).

C. Spring bloom phenology

Figure 11 shows the interannual variability of the spring blooms phenology. Fig. 11.A. shows the spring bloom onset date, fig. 11.B the date of maximum CHL, and fig. 11.C the total spring bloom duration, according to the year.

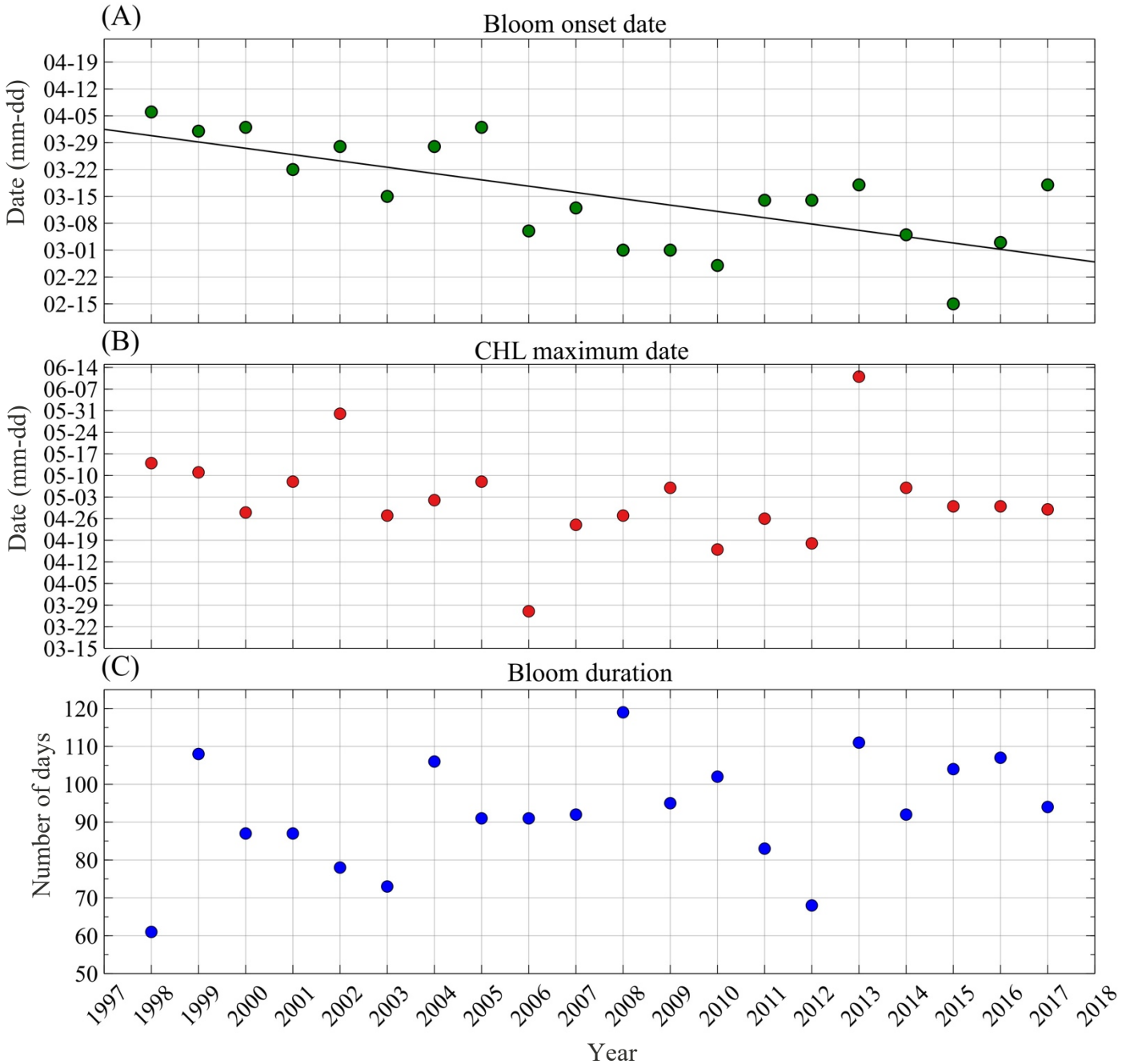

Figure 11 : Spring bloom phenology according to the years (1998 – 2017). (A) : bloom onset date according to the year; (B) : maximum CHL date; (C) : spring bloom duration. Spring bloom onsets and duration have been calculated according to a threshold method (eq. 1 and 2, section II.3.2.C). The solid black line represents a linear fit of the onset dates to the years, with R^2 = 0.5 and p-value = 0.00057.

Looking at fig. 11.A, we can see that, even if there is a strong interannual variability, there is a clear trend in the advancement of the spring bloom onset date with the years. It means that the spring bloom appears to start on earlier dates in the year. Our linear model indicates an advancement of about ~32 days between 1998 and 2017 (~1.6 days of advancement per year). This advancement of the onset dates in the year is significant (R^2 = 0.5 and p-value =.0.00057).

We also observe a slight advancement in the date of the maximum CHL (fig. 11.B), even though there is strong variability between years (with years 2006 and 2013 acting as outliers). This advancement is however not significant (p-value > 0.05) and is less important than the advancement in the date of the onset (a significant linear fit would indicate an advancement of 14 days in the date of maximum CHL between 1998-2017, if we consider 2006 and 2013 as outlier years). Therefore, even if the CHL maximum also appears to arrive earlier, it does not shift in time at the same rate as the onset date. The timing between the onset of the bloom and its maximum seems thus to increase with years.

The bloom duration shows a very strong interannual variability (fig. 11.C) and it is therefore difficult to establish a trend, even if it seems that bloom duration slightly increased during the period. Our linear model indicates that the slight increase observed is not significant and we must therefore be skeptical that bloom duration has increased over the period (R^2 =0.1235, p-value = 0.129).

Therefore, the overall trend regarding the spring bloom phenology is that blooms tend to onset earlier in the year (with ~1 month advancement between 1998 and 2017). The CHL maximum also occurs earlier, but not as significantly as the bloom onset. Concerning the total duration of the blooms, it is impossible to draw a trend, as it varies highly from year to year. The spring bloom is therefore shifting in time by arriving earlier in the year, with the shape of its signal being slightly modified (higher delay between the onset of the bloom and its maximum).

III.2. Abiotic variables

III.2.1. Suspended particular matter

Figure 12 shows the time series of the domain-averaged SPM (Fig. 12.A) as well as the key statistics (winter maximum, yearly mean, wintertime mean, summer minimum) of SPM according to the year (fig. 12. B).

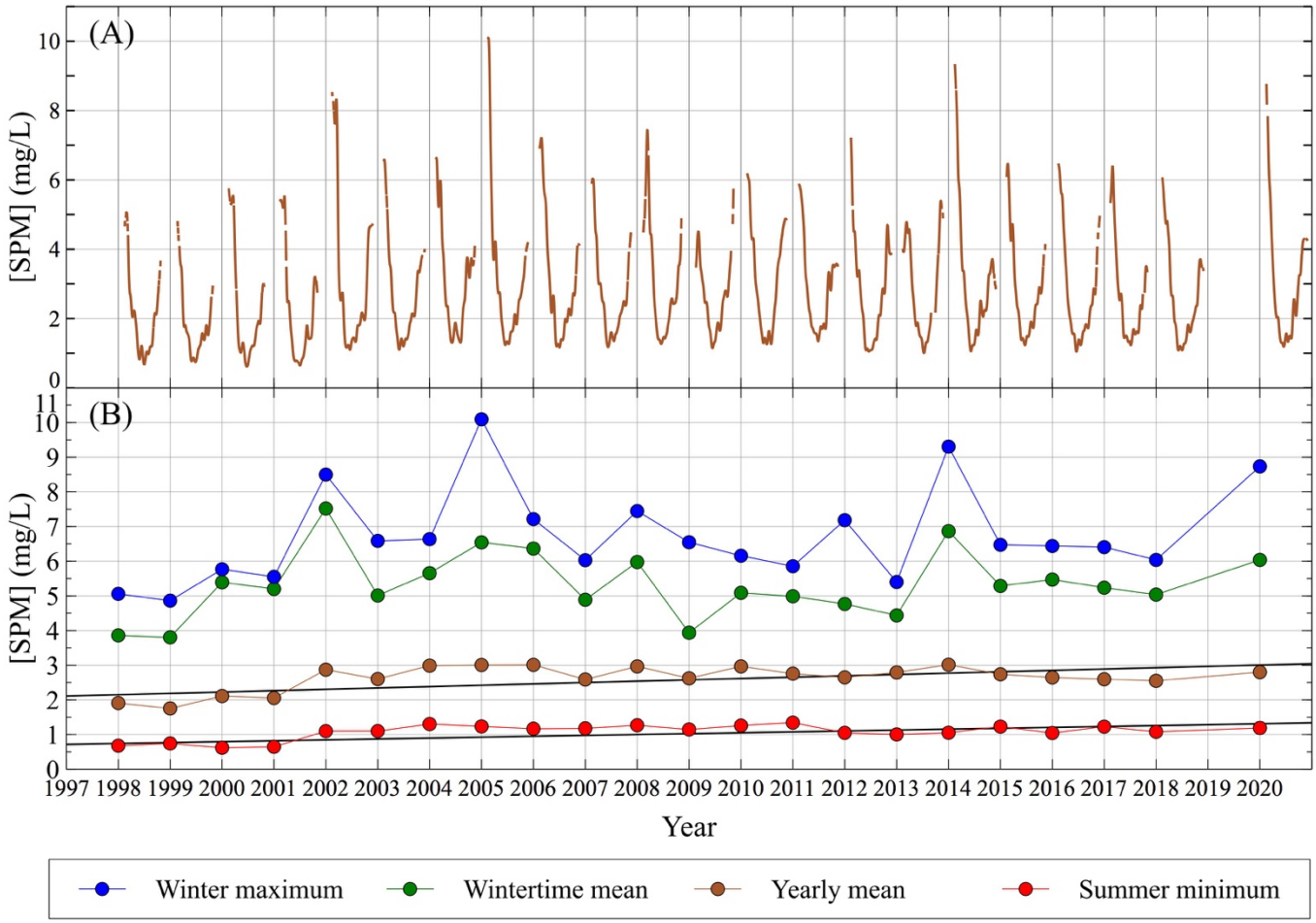

Figure 12 : Temporal variability of domain-averaged SPM over the 1998 – 2021 period (with year 2019 missing), in mg/L. (A) : domain-averaged SPM time series; (B) : SPM main statistics (winter maximum, summer minimum, wintertime and yearly means) according to the year. The wintertime means correspond to the domain-averaged SPM calculated between mid-February and the end of March. December – mid-February data are missing so wintertime and yearly means may be slightly underestimated. Solid black lines represent the linear fits of the yearly SPM means (R^2 = 0.3, p-value = 0.0128) and SPM summer minimums (R^2 =0.33, p-value = 0.008) to the years.

Looking at Figure 12.A., we can see that there is a very strong seasonality for the SPM for all years. The SPM is maximal in winter and decreases sharply to become minimal in summer, when vertical mixing and sediment resuspension is much lower. SPM winter maximum shows a

very high interannual variability (fig. 12.B). Years like 2002, 2005 and 2014 show very high winter maximum (the maximum of the SPM time series occurring in 2005 winter, 10.1 mg/L). This is reflected in their respective wintertime means, which also shows a strong interannual variability. Years 1998, 1999 and 2009 show the lowest SPM wintertime means (~ 3.9 mg/L) whereas year 2002 show the highest SPM wintertime mean (7.5 mg/L, fig. 12.B). There is no temporal trend observed over the period for both the winter maximum and means and these seem to have remained stable over the period (R^2 is close to 0 and the p-value >>0.05).

The SPM yearly mean offers less interannual variability. It increases significantly during the 1998 - 2017 period (R^2 = 0.3, p-value = 0.0128). According to the linear fit model, SPM mean has increased about 0.8 mg/L between 1998 and 2017. Similarly, the summer minimum also increased significantly during the study period (R^2 =0.33, p-value = 0.008). This increase seems to have taken place mainly during the period 1998 – 2004 (fig. 12. A).

Thus, SPM appears to have increased over the study period in the SNS. This increase is mostly reflected during the summer months, where the summer minimum significantly increased between 1998 and 2004. In contrast, the wintertime SPM appear to have remained relatively stable over the period.

III.2.2. Sea surface temperature

Figure 13 shows the time series of the domain-averaged SST (Fig. 12.A) as well as moving mean SST. The main statistics (maximum, minimum, yearly and wintertime mean) of SST according to the year are shown on fig. 13. B.

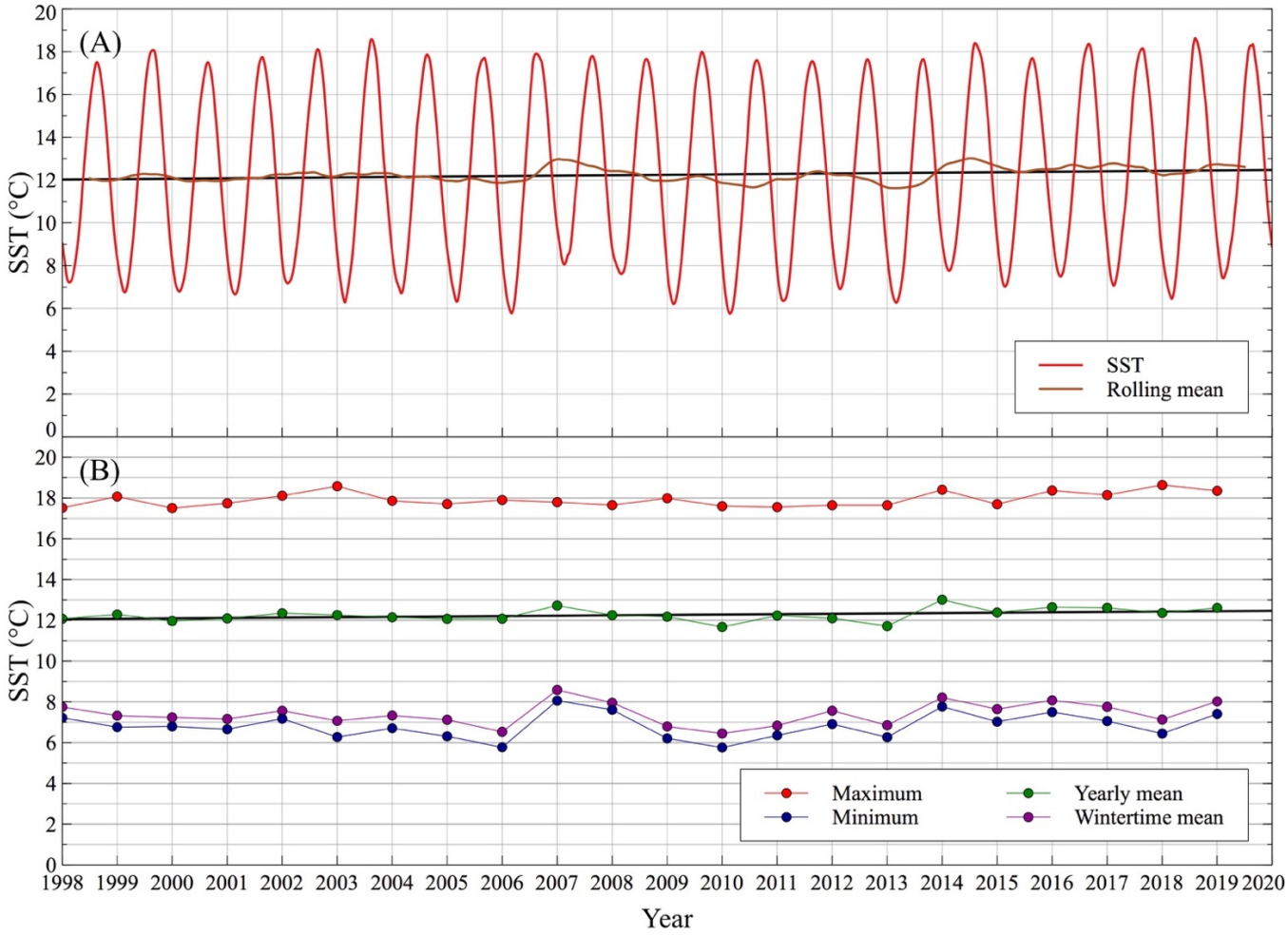

Figure 13 : Temporal variability of domain-averaged SST during the 1998 – 2020 period (°C). (A) : domain-averaged SST time series, as well as the SST moving means (with a 365-year window). Solid black line represents the linear regression of the SST moving means to the time (days), with R^2 =0.125 and p-value < 2.10^{-16}; (B) : SST main statistics (maximum, minimum, wintertime and yearly means) according to the year. The wintertime means correspond to the domain-averaged SST calculated between January and the end of March. Solid black line represents the linear fit of the SST yearly means (R^2 = 0.19, p-value = 0.45).

Not surprisingly, SST show a very marked seasonality, where temperatures oscillate between ~18°C (summertime maximum) and ~7°C (wintertime minimum) (fig. 13.A). To eliminate the seasonal signal and to retain the interannual variability, we need to look at the moving average (fig. 13.A, in dark orange). We can directly identify the warmer years (2007, 2014) as well as the colder years (2006, 2010, 2013). In spite of this interannual variability, we notice a trend of

increasing temperatures during the study period. Indeed, our linear fit model of the SST moving means to the time indicates that between 1998 and 2017, SST increased by 0.42°C (and 0.46°C between 1998 and 2019) and that this increase is significant (R^2 *=0.125 and p-value* < 2.10^{-16}). This trend is confirmed by the observed increase in the annual mean SST (fig. 13. B, green). When looking at the summertime maximum (fig. 13.B, red), it seems to slightly increase during the period. However, this cannot be confirmed by our linear regression analysis (p-value=0.075). On the other hand, no increasing trend can be found for the wintertime SST (p-value>>0.05), as well as the minimum SST (p-value>>0.05). In spite of their strong interannual variability, wintertime SST seem to have been stable through the period. Thus, the annual mean temperature seems to have increased over the period, but the summer month seems to have contributed more to this increase since winter temperatures have remained stable through the study period.

III.2.3. Precipitations

Figure 14 shows the yearly and the wintertime domain-averaged PPT mean (in mm/day), according to the year.

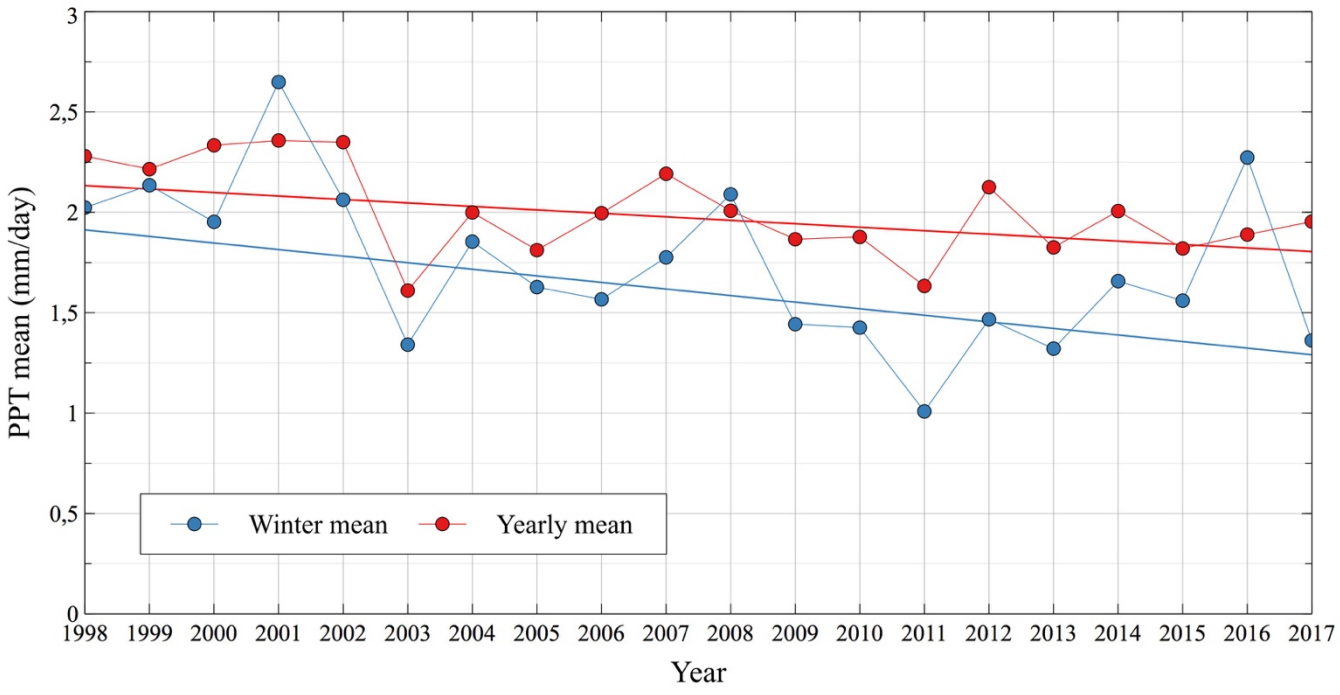

Figure 14 : Yearly and wintertime domain-averaged SST mean in function of the year between 1998 and 2017 (in mm/day). Solid blue line is a linear fit model of wintertime PPT mean to years (R^2 = 0.23, p-value = 0.031). Solid red line is a linear fit model of yearly PPT mean to years (R^2 = 0.3, p-value = 0.012).

We can observe a rather strong interannual variability, and especially for the wintertime means. Year 2001 and 2016 show the highest wintertime PPT mean and thus have been

particularly rainy during winter, whereas the winter of 2011 was particularly low in PPT (average 1 mm/day in winter). Regarding the yearly PPT mean, interannual variability is lower. The rainiest years over our domain were year 2000, 2001 and 2002 (~ yearly average of 2.35 mm/day), while year 2003 and 2011 show the lowest yearly PPT means (~1.6 mm/day). Despite the high interannual variability (especially for the wintertime PPT mean), there is strong evidence that precipitation has decreased during our study period. This is supported by our two linear regression models (p-value < 0.05), which shows a reduction of the yearly PPT average of 0.42 mm/day during the period. The reduction of the wintertime PPT is even greater, as it decreased by 0.65 mm/day between 1998 and 2017, according to the linear regression.

III.2.4. North Atlantic Oscillation

Because the meteorological conditions of the North-western Europe are mainly influenced by the wintertime NAO, we decided to retain only the wintertime NAO mean (NAO averaged between January-April). Figure 15 shows the wintertime NAO mean according to the year.

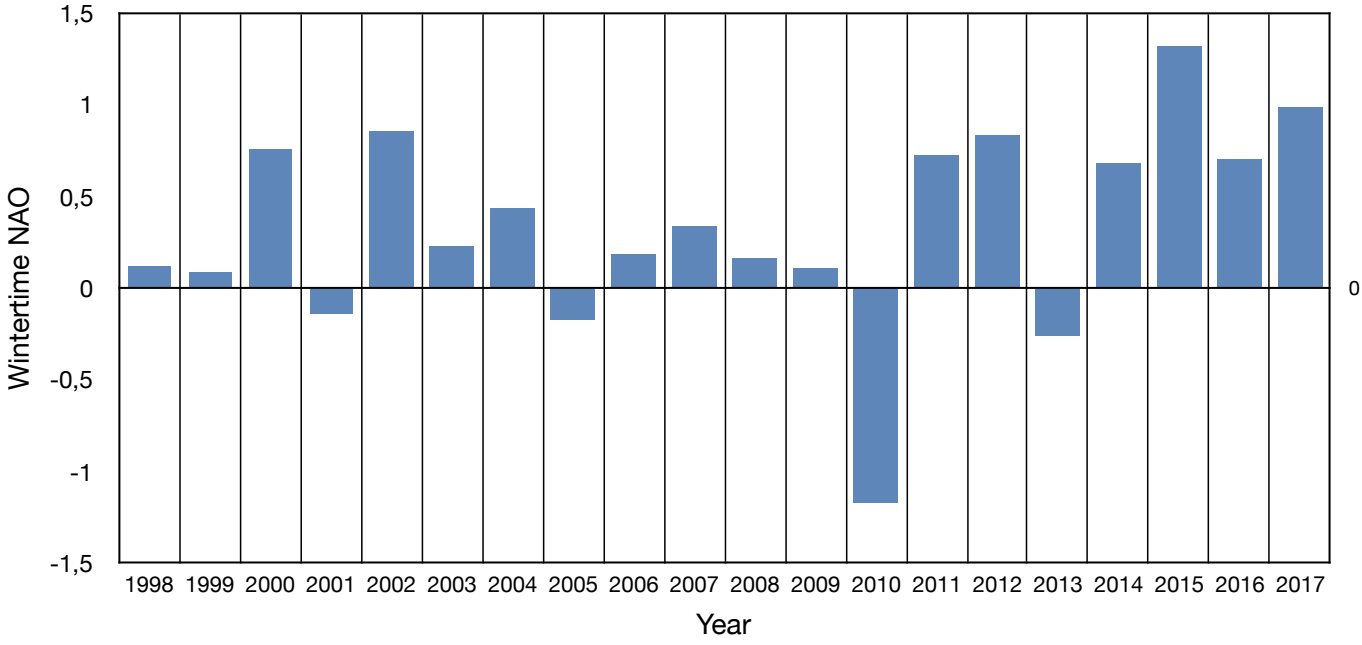

Figure 15 : wintertime-averaged NAO according to the year (1998-2017). The wintertime NAO mean represents the NAO averaged during January – April, for each year.

As seen in fig. 15, NAO wintertime mean shows a high year-to-year variability. Years like year 2002, 2012 or 2015 show a very high positive index, whereas year 2010 show a very negative one. Except for the years 2001, 2005, 2010 and 2013, all other years have positive

wintertime NAO mean. More broadly, the winter NAO appears to become increasingly positive over the period.

III.3. Correlation analysis

Figure 16 show us the correlogram plot of the Pearson's coefficient matrix between our retained variables, as explained in section II.3.7. The non-significant Pearson correlation coefficients (with a p-value of 0.05) have been crossed out.

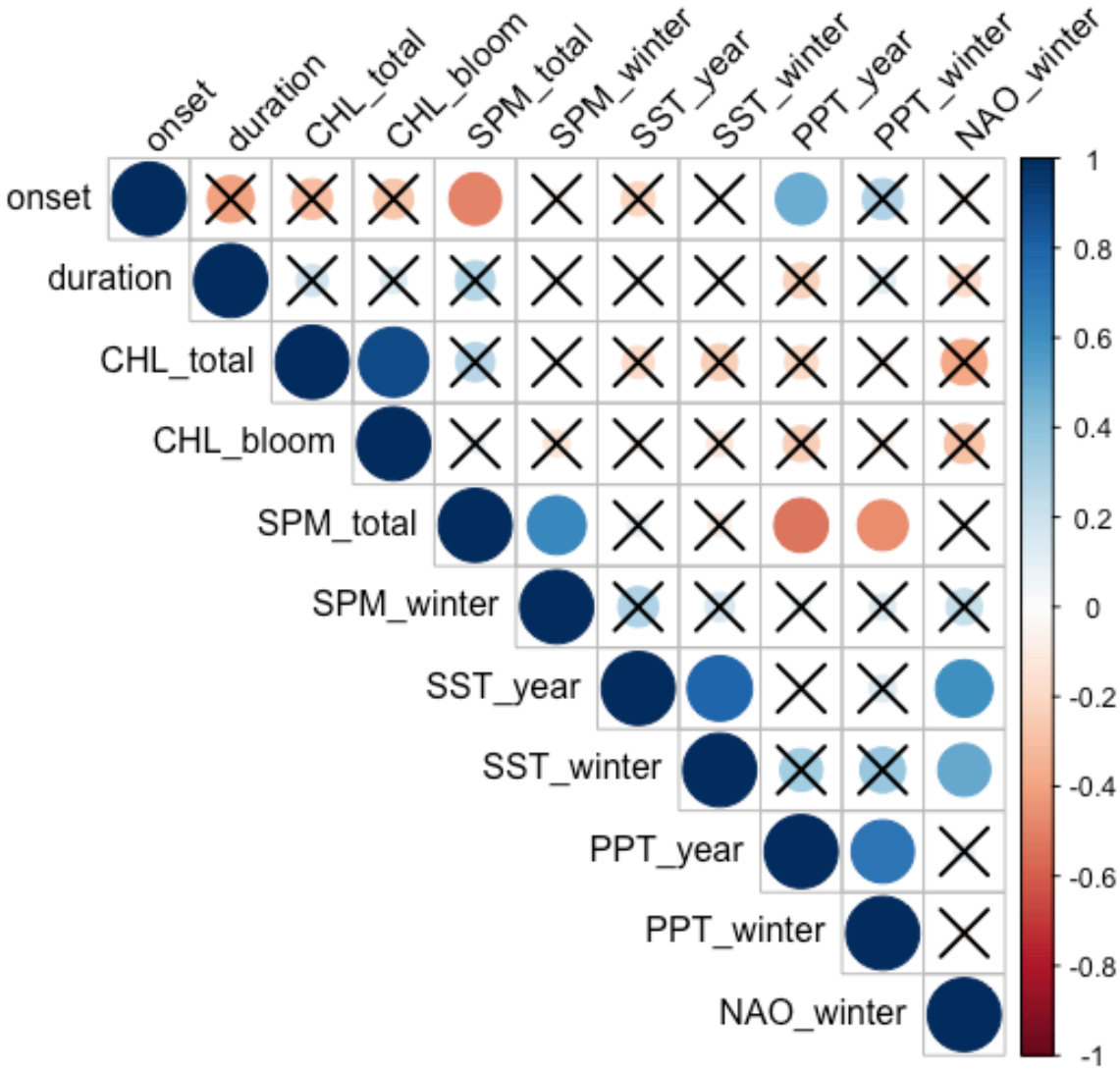

Figure 16 : Correlogram of the Pearson's coefficients between the retained variables. Blue circles indicate a positive correlation, where red circles indicate a negative one. The size of the circles as well as the color intensity represents the intensity of the correlation. Onset = onset date of the spring bloom ; duration : duration of the spring bloom ; CHL_total = CHL yearly mean ; CHL_bloom = CHL mean during the spring bloom ; SPM_total = SPM yearly mean ; SPM_winter = SPM mean during winter ; SST_year = SST yearly mean ; SST_winter = SST mean during winter ; PPT_year = PPT yearly mean ; PPT_winter = PPT mean during winter ; NAO_winter = NAO mean during winter. Unsignificant Peason's coefficients (with a p-value < 0.05) have been crossed out.

The onset date of the spring bloom is significantly negatively correlated with the SPM yearly mean, but not with the SPM winter mean. Conversely, it is positively correlated with annual PPT. This means that phytoplankton bloom should onset earlier during years with high average annual SPM but low precipitations.

Note also that onset date is slightly negatively correlated with SST yearly mean (although the correlation is not significant with our p-value), while it is not with SST winter mean (absence of correlation). This would indicate that winter temperatures may not have a strong influence on the spring bloom onset timing, where annual SST mean could have an influence. Bloom duration is not significantly correlated with any variable, probably because it has too much interannual variability.

Even if the CHL yearly mean and CHL bloom mean are not significantly correlated to any variable, we note that they could be negatively correlated with the NAO winter mean when lowering our interval confidence (p-value = 0.1). This would mean that years with a strong NAO positivity during winter show lower CHL, both annually and during the spring bloom.

Surprisingly, SPM annual means (but not wintertime means) are significantly negatively correlated with yearly and wintertime PPT means. This means that years with higher PPT show lower SPM, and inversely.

Finally, SST yearly and wintertime means show significant positive correlations with NAO winter mean. This shows that years with a strongly positive NAO during winter show higher SST during the year and the winter.

CHAPTER IV : DISCUSSION

IV.1. Abiotic variables

IV.1.1. Suspended particulate matter

Light availability is an important factor for phytoplankton growth and phenology. High SPM reduce the radiation available for photosynthesis. For this reason, SPM and water turbidity are often considered as a determining factor in the phytoplankton dynamics and the onset of the bloom (Desmit et al., 2015; Opdal et al., 2019).

Our results pointed out an increase in SPM in the North Sea over the study period (0.042 mg/L.year), with a particularly marked increase during the period 1998 – 2004 (fig. 12). This increase seems to be more significant during summer months than during winter. These results are in agreement with the studies of (Capuzzo et al., 2015, 2018) which showed a general increase in the water turbidity of the SNS during the last century, as well as the two last decades. Similarly, with their model, Opdal et al. (2019) showed that turbidity increased about 5-fold during the 20th century in the SNS, and suggested that this increase was related to the browning of the surface waters coming in the SNS. Wilson & Heath (2019) also showed that SPM increased in the NS during the 20th century. However, they suggested with their hindcasts of wave and current data that SPM increased in the NS because of the increased sediment resuspension induced by the greater wave-induced bed shear stress (which particularly increased in the SNS over the last century). According to our results, SPM is negatively correlated with PPT. We conclude that the observed increase of SPM in our study is probably more due to an increased turbulent mixing than an increase in riverine SPM inputs, as these inputs should decrease with less PPT. The increased turbulent mixing could probably due to higher wind speeds during the period, as suggested by our increased NAO positivity. Capuzzo et al. (2015) also concluded that one of the main reasons for an increase of the turbidity could be due to the increased sediment resuspension, and that this increased resuspension was probably linked to the higher wind speeds driven by a higher NAO positivity. It would have been interesting to study the changes in wind intensity in the SNS during the same period.

IV.1.2. Sea surface temperature

SST, in addition to potentially affecting the water stratification regime in more open waters, can also influence the cell division rate of the phytoplankton (Desmit et al., 2020; Høyer & Karagali, 2016; Hunter-Cevera et al., 2016). Similarly, a regime shift in the SST can strongly affect phytoplankton communities and the timing of spring bloom (Alvarez-Fernandez & Riegman, 2014; Desmit et al., 2020; Hunter-Cevera et al., 2016; Lohmann & Wiltshire, 2012; Weijerman et al., 2005).

There is a clear evidence of an increasing trend of the SST in the North Sea these last decades (Capuzzo et al., 2018; Desmit et al., 2020; Edwards et al., 2002; Høyer & Karagali, 2016; van Aken, 2010; Karen H. Wiltshire et al., 2015; Karen H. Wiltshire & Manly, 2004). This is in agreement with our analysis, which highlighted an increase of ~0.021°C/year in average during the 1998 – 2017 period over our domain. This increase is slightly higher than the 0.015°C/year increase observed by Alvera-Azcárate et al., (2021) over the Greater NS domain (which used the same SST product as us). This result indicates that the southern part of the NS is more sensitive to this warming trend. This is consistent with the regime shift observed during these two last decades in the NS, which are characterized by a significant inflow of warmer and saltier Atlantic waters through the channel into the SNS (Alvarez-Fernandez et al., 2012; Desmit et al., 2020; Edwards et al., 2002; Weijerman et al., 2005).

Even if our observed increase is significant, it is lower than the increase found by Desmit et al. (2020) (~ 0.035°C/year, which used in-situ data during the 1971 – 2014 period), by Wiltshire et al (2010) (~0.037°C, which used 1962 – 2007 time series of in-situ observations at Helgoland Roads in the Wadden sea) and the one found by Hoyer et al. (2016) (0.037°C/year, using a reanalysis product during the 1982 – 2012 period). However, the time period, the domain investigated, as well as the methods used are not the same, so these results are not directly comparable. In this respect, it is likely that SST increased more strongly in the later years of the 2nd millennium, which coincides with the beginning (1998) of the regime shift in the SNS (Desmit et al., 2020), than during our study period. It is difficult to determine whether this trend of temperature increase is due to climate change or to natural meteorological oscillations such as the NAO. Our results pointed out a strong correlation between the wintertime-averaged NAO and SST. This was also observed in the study of Wiltshire et al., (2009), indicating that the increase of SST is strongly related to the increase of wintertime NAO. While not investigated during our study, Wilsthire et al. (2009) have also shown that the number of winter days with a SST

conducive to algal growth (i.e. > 5°C) have increased significantly between 1962 and 2007. This could have had an important consequence on the timing of the bloom onsets.

IV.1.3. Precipitations

While PPT may not appear as important as the other variables, high PPT could increase the amount of riverine nutrient inputs to the SNS. In addition, high PPT may locally impact the stratification/mixing regime, as well as the salinity.

Our results showed both a significant decrease in annual as well as wintertime PPT between 1998 and 2017 over the study area. This decrease in PPT could have resulted in a decreased amount of leached nutrients ending up in the coastal areas, and thus accentuated the de-eutrophication trend observed in the SNS (Desmit et al., 2020)

This decrease in PPT was not correlated with the NAO, which has increased over the period. A higher NAO corresponds to a wetter winter in Europe and increased PPT (Rousseau et al., 2008). Thus, this decrease in PPT is surprising. It is possible that the low resolution of our PPT product (2.5° x 2.5°) did not allow a good enough accuracy to correctly assess the PPT temporal trend over our domain.

IV.1.4. North Atlantic Oscillation

As a reminder, the NAO measures the large-scale gradient between the Icelandic Low and the Azores High pressures. It is highly correlated with the northern Europe climatic conditions (Hernández-Fariñas et al., 2014; V. Rousseau et al., 2008; Thomas et al., 2018; Zhai et al., 2013). It has also a strong influence on the SNS meteorological and hydrological conditions. In periods of high NAO, southwesterly winds are dominant and stronger, driving a stronger inflow of warmer Atlantic waters from the English Channel into the SNS. High NAO thus often coincides with higher SST and salinity in the SNS waters. A high NAO is also often correlated with increased PPT, impacting the delivery of nutrients in the SNS (Rousseau et al., 2008).

Our results showed that the wintertime-averaged NAO increased during our study period (Fig. 15). Interestingly, PPT over the domain decreased and no correlation was found between winter NAO and PPT (Fig. 16). This increased wintertime NAO positivity during the last two decades has already been documented by several authors and have been identified as the main factors explaining the regime shift which has occurred in 1998 in the SNS (Desmit et al., 2020;

Llope et al., 2009; Lohmann & Wiltshire, 2012; Peperzak & Witte, 2019; Weijerman et al., 2005; Karen Helen Wiltshire et al., 2009).

In addition to having a strong impact on meteorological and hydrological conditions, numerous studies have established a link between a NAO change and a shift in phytoplankton bloom dynamics and communities (Alvarez-Fernandez et al., 2012; Beaugrand, 2004; Beaugrand & Ibanez, 2004; Hernández-Fariñas et al., 2014; Peperzak & Witte, 2019; Sharples et al., 2006; Ueyama & Monger, 2005; Weijerman et al., 2005; Karen Helen Wiltshire et al., 2009; Zhai et al., 2013).

For example, a cold episodic event related to the NAO occurred in the SNS in the late 1970s (Alvarez-Fernandez et al., 2012; Desmit et al., 2020). In their study, Edwards et al. (2002) explained how during this cold SST period spring blooms were smaller and occurred later in the year. They also observed that many phytoplankton species (mostly diatoms and dinoflagelletes) were absent from the blooms, indicating a shift in the planktonic community (Alvarez-Fernandez et al., 2012). Similarly, Lohmann & Wiltshire (2012) studied the phenology of winter-blooms of diatoms in the Wadden Sea. They observed that the diatom blooms tended to occur earlier when the atmospheric circulation allowed an increased inflow of warmer Atlantic waters into the North Sea. On the contrary, the bloom was occurring later when a more continental atmospheric flow coming from the east was observed.

IV.2. Spatial variability of CHL

Our results indicate that there is a wide spatial variability of CHL in the SNS. Still, a general pattern can be stated from fig. 7: CHL typically show a strong coastal-offshore decreasing gradient. Highest CHL are mainly located along the coastline of northwestern Europe (French, Belgian and Dutch coastal zones) and the east coastline of United-Kingdom, with mean annual values greater than or equal to 10 µg Chl/L. Coastal areas of the SNS receive a constant supply of nutrients coming from the nutrient-enriched rivers. Along with the very well-mixed environment encountered in coastal areas (low bathymetry and strong tidal energy) (Desmit et al., 2015, 2020), this creates ideal conditions for the phytoplankton to develop intensively, even during summer and fall seasons (C Lancelot et al., 2005; Chrisitane Lancelot et al., 1997; Philippart et al., 2010; Reid et al., 1990; V. Rousseau et al., 2008). This is what we observe in fig. 8, where coastal zones still show moderate – high CHL during July-August, whereas offshore waters have very low concentrations.

To address the long-term (~30-50 years) changes which could have occurred in the phytoplankton bloom dynamics, we compared our results with the review done by Reid et al. (1990), which compiled series of phytoplankton dynamics and CHL data during the 1970s in the Belgian and Dutch coastal zone. With their montly climatologies calculated during the 1974 – 1979 period, they also showed an important CHL gradient between coastal and offshore waters. One notable difference is that our highest CHL means in the SNS are observed in April, while theirs are observed during June, with May having lower concentrations than April and June. It might be possible that Reid et al. missed part of the bloom, due to sampling limitations. It is also possible that this bimodal (small bloom in April and high bloom in June) dynamic observed in the 1970s has shifted to a single intense spring bloom occurring in April-May in more recent years, as observed in (Philippart et al., 2010; Nohe et al., 2020). In addition, our concentrations appear to be lower than theirs (their concentrations during the growing season reach 20 - 25 microg/L while ours remain below 15 microg/L), meaning that CHL were probably higher during the 1970s than during these 2 last decades. During this period, nutrient concentrations were probably higher because the eutrophication process was a less known phenomenon and the OSPAR was not implemented yet.

Our results seem more consistent when comparing them to a more recent study. Xu et al. (2020) used a coupled high-resolution 3D-physical-biogeochemical along with in-situ observations to assess the spatial and temporal evolution of phytoplankton between 1987 and 2012 in the SNS. They found temporal-averaged CHL means of about ~ 10 µg Chl/L all along the coastline of France, Belgium and the Netherlands, while CHL means in the offshore waters of the SNS are around 3-4 microg/L. Interestingly, they noted that chlorophyll concentrations in their coastal areas increased by about 20% during their study period, while the open waters showed the opposite trend, with an average decrease of 10%. This highlights a first limitation of our study: the evaluation of temporal changes was performed over the entire domain, which does not allow us to evaluate the different temporal trends according to regions with very different conditions (e.g. coastal waters vs. offshore waters).

IV.3. Temporal variability of CHL

IV.3.1. Seasonal dynamics

Fig. 9 shows us that at the scale of the SNS basin, there is a strong spring bloom dynamic. We also see two flattened signals in mid-summer and late summer. These signals are certainly the result of the summer blooms that can take place in the coastal zones, as can be seen in fig. 8, where CHL in July and August remain relatively high along the coast. These signals may appear weak (fig. 9), but it should be kept in mind that the CHL time series has been averaged over the entire domain.

Philippart et al. (2010) analyzed long-term field observations of CHL during the 1974 – 2007 period in the western Wadden Sea. Their interpolation model of the CHL seasonality coming from in-situ CHL observations coincides well with our strong spring bloom signal shape. Interestingly, they highlighted a fading of the late summer/autumn bloom during their period of study. The same phenomenon was observed by (Muylaert et al., 2006; Nohe et al., 2020) which pointed out that the diatom bloom pattern changed from a bimodal (spring and autumn) mode in the 1970s to a more extended unimodal spring-summer bloom in the 2000s in the Belgian part of the SNS.

Some of the drivers for such fading of the late-summer bloom could be the increase in late summer SPM and SST (fig. 12 and fig. 13, respectively), conjointly with the nutrient inputs reduction (Desmit et al., 2020). Higher SPM during late SPM might limit light availability, whereas higher SST during summer and fall may induce an increased grazing pressure, thus limiting the development of late-summer blooms (Phillippart et al., 2010).

IV.3.2. Interannual changes

A. Chlorophyll concentrations

Several authors have investigated long-term trends in CHL and primary production in the SNS. Since the 1970s, both increases and decreases in phytoplankton biomass have been reported in different parts of the North Sea (Alvarez-Fernandez & Riegman, 2014; Capuzzo et al., 2015, 2018; Desmit et al., 2020; Joint & Pomroy, 1993; McQuatters-Gollop et al., 2007; Anja Nohe et al., 2020). Such conflicting trends may be caused by methodological differences, but also reflect the strong environmental differences related to the different regions investigated (bathymetry, hydrodynamics, climate, riverine and Atlantic influence, etc.) (Nohe et al., 2020).

Using satellite data at the scale of the SNS during the 1998 – 2017 period, our results showed different trends according to the period considered. CHL increased from 1998 to 2003, then remained stable until 2014, after which it decreased until 2017 (fig. 10 A,B). Satellite CHL time series of Alvera-Azcárate et al. 2021 indicate that CHL remain stable during 2017 – 2020 over the Greater North Sea. In their study, Desmit et al., (2020) used in-situ measurements and observed a decline in the yearly mean of CHL at 11 out of 18 sampling sites (coastal and offshore) during the 1988 – 2016 period. Capuzzo et al. (2017), which analyzed time-series of primary production and in-situ measurements of CHL and turbidity from 1988 to 2013, concluded in a decline in CHL and net-primary production. They attributed this decline to the increased water turbidity observed during the period, as well as the decreasing nutrients concentrations.

Factors influencing CHL which could explain interannual variability are numerous, such as temperature, nutrient concentrations, water turbidity (SPM) and/or light availability (Alvera-Azcárate et al., 2021; Desmit et al., 2020). However, phytoplankton total and maximum biomass are mainly determined by nutrient concentrations. In response to the various measures taken by the OSPAR Convention and the subsequent decrease of dissolved nutrient concentrations in rivers feeding the North Sea a decrease of the average CHL in SNS waters should be expected (Desmit et al. 2020). Our results only show a significant decrease in concentrations from 2014 onwards. The effects of nutrient reductions such as N on marine ecosystems may take several years, or even decades, after their implementation due to retention of N in soils and aquifers (van Grisven 2011). Thus, effects of nutrient reduction may not be directly visible and could be strongly delayed.

B. Spring bloom phenology

Different factors such as temperature, light availability, hydrographical conditions, nutrient availability and grazing may affect the phenology of marine phytoplankton. Even if light availability and water temperature are often considered as being the main driving factors, the relative importance of the drivers of phytoplankton phenology on the regional scale is likely to be variable in space (Scharfe & Wiltshire, 2019).

The most compelling result of our study is that between 1998 and 2017, the spring bloom arrives over 1 month earlier in the year in the SNS. Several authors have investigated the phenology of phytoplankton blooms in the North Sea. Desmit et al. (2020), which investigated long-term series of in-situ CHL observations between 1970 and 2010, showed an important advancement in the spring bloom onset date at various locations of the SNS since the early 2000s. Philipart et al. (2010), which analyzed long-term field observations of CHL during 1974 –

2007, showed on the contrary no trend in the timing of the phytoplankton spring blooms. However, since their study was limited to only one sampling point in the Wadden Sea, it is not able to represent the variability that is observable over the entire SNS domain with satellite data. Alvera-Azcárate et al. (2021) demonstrated the same shifting trend in the spring bloom onset timing using satellite CHL data in the Greater North Sea domain. Their observed advancement rate is about 1.5 days/year in the domain, which is a slightly lower rate than ours (1.6 days/year). This may indicate that the phenological shift in the spring blooms timing is more important in the southern part of the NS.

An increase in water temperature could trigger earlier blooms. This has already been shown in lakes (Peeters et al., 2007) and in ocean (Winder & Sommer, 2012). In the same logic, a better availability of light (following a decrease in turbidity, for example) could trigger blooms earlier (Capuzzo et al., 2017; Desmit et al., 2020; Leynaert et al., 2002). However, our results indicate a negative correlation between the onset of the bloom and total SPM, which is rather inconsistent. In addition, the onset date of the bloom is not correlated with the wintertime SPM. We therefore believe that the SPM did not play a direct role on the timing of the onset by acting on the light availability.

Our results also show that SST significantly increased in the SNS by about 0.42°C between 1998 and 2017. In their studies, (Desmit et al., 2020; Hunter-Cevera et al., 2016) proposed that increased SST temperature during winter and early spring might promote earlier bloom by stimulating the phytoplankton cell division. This is not consistent with our findings because, although the mean annual SST increased over the period, the mean SST during winter (January - March) did not increase significantly, according to our results.

While the timing of bloom onset is not correlated with wintertime SST, it is possible that the observed long-term temperature increase has altered planktonic communities in the SNS. Such a change in the planktonic regime has already been observed in the NS several times before (1979, 1987), and the main driver for these regime shifts was a change in water temperatures (Alvarez-Fernandez et al., 2012; Beaugrand, 2004; Desmit et al., 2020; Edwards et al., 2002; Weijerman et al., 2005). Some authors also pointed out a regime shift occurring in 1998 in the SNS driven by increased SST and higher Atlantic waters inflow (Alvarez-Fernandez et al., 2012; Werijerman et al., 2005 ; Desmit et al .2020). The regime shift observed in 1998 is consistent with the increase of annual SST and wintertime NAO that we observed since 1998.

Sommer & Lewandoska (2011) investigated the effect of water warming on the timing of spring bloom onset by in-situ mesocosm studies. They conclude that the warming induced

changes in the dynamic of the phytoplankton spring bloom cannot be understood without considering grazing by the zooplankton. In their study, Alvarez-Fernandez et al. (2012) found out that the 1998 regime shift impacted the abundance and the seasonal patterns of the dominant zooplankton group. They noticed that the relative abundance of neritic cold-water copepods dropped during this regime. It is therefore likely that the decrease in the abundance of cold-waters copepods resulted in a decrease in the grazing rate of winter-blooming diatoms during winter. This could allow these winter diatoms to develop more readily during the winter, which could explain why we have an advancement in the bloom onset and why we observe higher CHL during late winter. This supposition would be coherent with the study of (Lohmann & Wiltshire, 2012) which have already shown that higher SST and higher Atlantic water inflows may have caused an earlier onset of winter diatom blooms in the NS.

In addition to the change in zooplanktonic communities, the WFD and the MSFD resulted in a reduction of P and N inputs in the SNS. Furthermore, Desmit et al. (2015) noticed a strong increase in silica (Si) river-borne inputs in the SNS during 1990 – 2007 period. In consequence, Si/N and Si/P ratio may have strongly increased in the SNS. This increase may have further favored siliceous diatoms at the expense of less-siliceous species such as *Phaeocystis globosa*, which is more dependent to excessive N and P concentrations (Gypens et al., 2007; Lancelot et al., 2005; Nohe et al., 2020). Similarly, the observed decreasing trend of the annual and winter PPT observed during the period could have also contributed to a decrease in nutrient inputs in the SNS, thus limiting the competitive advantages of opportunistic species such as *Phaeocystis* and favoring the emergence of winter blooms.

We therefore propose here that the observed advance in phytoplankton bloom onset is a direct result of a SST-driven shift in the zooplankton communities in the SNS, inducing a lower rate of grazing towards winter diatoms. This change in grazing regime, in combination with the de-eutrophication trend and the increased river-bone Si inputs, could favor the emergence of late-winter diatom blooms, thus explaining why we observe higher CHL during this time of the year.

This proposal is purely speculative as we had neither nutrient concentrations nor planktonic community composition data. It would have been interesting to integrate the monitoring of N, P and Si concentrations in this study, to confirm or refute these assumptions. Similarly, data on planktonic communities over the period could have helped us determine whether or not this advancement in the onset date is due to conditions favoring the emergence of winter diatom blooms.

CHAPTER V : CONCLUSION

The purpose of this master thesis was to assess the long-term changes in the eutrophication status of the SNS using gap-free satellite products with a long temporal coverage (1998-2017). The satellite data were able to highlight year-to-year as well as long-term changes in phytoplankton dynamics over our period of study. Our results showed that CHL (a proxy for phytoplankton biomass) increased during 1998 – 2004, stagnate, then decrease from 2014 – onwards. This recent decrease in CHL is probably an early consequence of the different measures taken by the OSPAR Convention to limit the input of nutrients in the SNS (Alvera-Azcárate et al., 2021).

In parallel to this, our study pointed out that there has been a phenological shift of approximately 1 month in the onset date of the spring blooms in the SNS. Our study also revealed a significant increase in SPM as well as SST, positively correlated to the wintertime NAO. Surprisingly, PPT decreased during the period, but this may be due to the poor spatial resolution of the PPT product used.

While it is difficult to identify a particular factor responsible for the phenological shift, the SNS has undergone significant changes in its climatic regime over the past 20 years and this is supported by our results. This change in meteorological conditions seem to have occurred in 1998 (Alvarez-Fernandez et al., 2012; Desmit et al., 2020; Edwards et al., 2002; Weijerman et al., 2005) and has mainly led to higher SST as well as higher Atlantic waters inflow in the SNS. Such a change in the NS regime has already been shown in the past to have a major importance on phytoplankton, causing a change in planktonic communities and/or phenology (e.g. Sharples et al., 2006; Weijerman et al., 2005). It is unfortunate that our satellite data did not extend before 1998, which would have allowed us to observe this shift.

Based on what we found in the literature, we assume that this regime shift, combined with a de-eutrophication trend, may have altered zooplanktonic communities and subsequent grazing conditions(Alvarez-Fernandez et al., 2012), favoring the development of late-winter blooming species such as diatoms (Lohmann & Wiltshire, 2012). This could explain why we observe a phenological shift in the blooms in the SNS, occurring earlier in the year.

The results of this study showed that they were consistent with the results of other authors who used different methods (e.g. in situ data or models). We therefore believe that the use of gap-free satellite products offers an excellent tool to monitor different variables related to eutrophication such as CHL, SPM or SST, over a wide spatial and temporal coverage. However, our study still encountered limitations:

First, the use of satellite data implies that we only have information on the first meter of the water column. If the SNS is a relatively well-mixed sea, it doesn't allow us to explore the vertical heterogeneity that we could have in the more open waters of our domain.

Second, our study and analyses were carried out at the scale of the entire SNS by considering it as a single object, while it has a significant spatial heterogeneity in terms of hydrological and environmental conditions (e.g. English Channel vs. Southern Bight, coastal regions vs. offshore waters, etc.). This spatial heterogeneity makes the phytoplankton dynamics and eutrophication trends highly variable between regions. In the future, it would be important to sub-divide the domain into regions according to their characteristics to investigate possible signals that may have been missed in our study due to the domain averaging.

Third, our statistical analyses consisted mainly in the use of simplistic linear correlation coefficients. These linear correlations may not be suitable for monitoring an environmental system as complex as the SNS, where many variables may not respond in a linear way. In addition, our linear relationship analyses do not take into account possible synergistic or antagonistic interactions between different variables.

Finally, our study did not include any in-situ measurements of variables that are essential in the evaluation of the eutrophication of an environment, such as the measurement of nutrients, phytoplanktonic composition, dissolved oxygen, or even pH. This can limit the interpretation and the possible interpolation of the results.

In the future, it would be interesting to complement our satellite data with in-situ analyses to assess long-term changes in the ecosystems. In this respect, it would be particularly interesting to monitor nutrient concentration levels (N, P, Si) as well as to characterize the composition and succession of spring phytoplankton blooms in the SNS to see if the observed phenological shift is effectively due to the emergence of late-winter blooming diatoms.

CHAPTER 6 : REFERENCES

Allan, M. G. (2008). Remote Sensing of Water Quality in Rotorua and Waikato Lakes (Thesis, Master of Science (MSc)). The University of Waikato, Hamilton, New Zealand. Retrieved from https://hdl.handle.net/10289/2292

Alvarez-Fernandez, S., Lindeboom, H., & Meesters, E. (2012). Temporal changes in plankton of the North Sea: community shifts and environmental drivers. *Marine Ecology Progress Series*, *462*, 21–38. https://doi.org/10.3354/MEPS09817

Alvarez-Fernandez, S., & Riegman, R. (2014). Chlorophyll in North Sea coastal and offshore waters does not reflect long term trends of phytoplankton biomass. *Journal of Sea Research*, *91*, 35–44. https://doi.org/10.1016/J.SEARES.2014.04.005

Alvera-Azcárate, A., Barth, A., Rixen, M., & Beckers, J. M. (2005). Reconstruction of incomplete oceanographic data sets using empirical orthogonal functions: Application to the Adriatic Sea surface temperature. *Ocean Modelling*, *9*(4), 325–346. https://doi.org/10.1016/j.ocemod.2004.08.001

Alvera-Azcárate, A, Barth, A., Sirjacobs, D., & Beckers, J.-M. (2009). Enhancing temporal correlations in EOF expansions for the reconstruction of missing data using DINEOF. In *Ocean Sci* (Vol. 5). www.ocean-sci.net/5/475/2009/

Alvera-Azcárate, Aida, van der Zande, D., Barth, A., Troupin, C., Martin, S., & Beckers, J.-M. (2021). Analysis of 23 years of daily cloud-free chlorophyll and suspended particulate matter in the Greater North Sea. *Frontiers in Marine Science*, *Ocean Observation*, 1276. https://doi.org/10.3389/FMARS.2021.707632

Arkin, Phil, Xie, PIngping & National Center for Atmospheric Research Staff (Eds). Last modified 17 Apr 2020. "The Climate Data Guide: CMAP: CPC Merged Analysis of Precipitation ." Retrieved from https://climatedataguide.ucar.edu/climate-data/cmap-cpc-merged-analysis-precipitation.

Banks, A. C., Prunet, P., Chimot, J., Pina, P., Donnadille, J., Jeansou, E., Lux, M., Petihakis, G., Korres, G., Triantafyllou, G., Fontana, C., Estournel, C., Ulses, C., & Fernandez, L. (2011). *A satellite ocean color observation operator system for eutrophication assessment in coastal waters*. https://doi.org/10.1016/j.jmarsys.2011.11.001

Barnston, A. G., & Livezey, R. E. (1987). Classification, Seasonality and Persistence of Low-Frequency Atmospheric Circulation Patterns. *Monthly Weather Review*, *115*(6), 1083–1126. https://journals.ametsoc.org/view/journals/mwre/115/6/1520-0493_1987_115_1083_csapol_2_0_co_2.xml

Beaugrand, G. (2004). The North Sea regime shift: Evidence, causes, mechanisms and consequences. In *Progress in Oceanography* (Vol. 60, Issues 2–4, pp. 245–262). Elsevier Ltd. https://doi.org/10.1016/j.pocean.2004.02.018

Beaugrand, G., & Ibanez, F. (2004). Monitoring marine plankton ecosystems. II: Long-term changes in North Sea calanoid copepods in relation to hydro-climatic variability. *Marine Ecology Progress Series*, *284*, 35–47. https://doi.org/10.3354/MEPS284035

Beckers, J. M., & Rixen, M. (2003). EOF calculations and data filling from incomplete oceanographic datasets. *Journal of Atmospheric and Oceanic Technology*, *20*(12), 1839–1856. https://doi.org/10.1175/1520-0426(2003)020<1839:ECADFF>2.0.CO;2

Brody, S. R., Lozier, M. S., & Dunne, J. P. (2013). A comparison of methods to determine phytoplankton bloom initiation. *Journal of Geophysical Research: Oceans*, *118*(5), 2345–2357. https://doi.org/10.1002/jgrc.20167

Capuzzo, E., Lynam, C. P., Barry, J., Stephens, D., Forster, R. M., Greenwood, N., McQuatters-Gollop, A., Silva, T., van Leeuwen, S. M., & Engelhard, G. H. (2017). A decline in primary production in the North Sea over 25 years, associated with reductions in zooplankton abundance and fish stock recruitment. *Global Change Biology*, *24*(1), e352–e364. https://doi.org/10.1111/gcb.13916

Capuzzo, E., Lynam, C. P., Barry, J., Stephens, D., Forster, R. M., Greenwood, N., McQuatters-Gollop, A., Silva, T., van Leeuwen, S. M., & Engelhard, G. H. (2018). A decline in primary production in the North Sea over 25 years, associated with reductions in zooplankton abundance and fish stock recruitment. *Global Change Biology*, *24*(1), e352–e364. https://doi.org/10.1111/GCB.13916

Capuzzo, E., Stephens, D., Silva, T., Barry, J., & Forster, R. M. (2015). Decrease in water clarity of the southern and central North Sea during the 20th century. *Global Change Biology*, *21*(6), 2206–2214. https://doi.org/10.1111/gcb.12854

Claussen, U., Zevenboom, W., Brockmann, U., Topcu, D., & Bot, P. (2009). Assessment of the eutrophication status of transitional, coastal and marine waters within OSPAR. *Hydrobiologia*, *629*(1), 49–58. https://doi.org/10.1007/978-90-481-3385-7_5

Desmit, X., Nohe, A., Borges, A. V., Prins, T., de Cauwer, K., Lagring, R., van der Zande, D., & Sabbe, K. (2020). Changes in chlorophyll concentration and phenology in the North Sea in relation to de-eutrophication and sea surface warming. *Limnology and Oceanography*, *65*(4), 828–847. https://doi.org/10.1002/lno.11351

Desmit, X., Ruddick, K., & Lacroix, G. (2015). Salinity predicts the distribution of chlorophyll a spring peak in the southern North Sea continental waters. *Journal of Sea Research*, *103*, 59–74. https://doi.org/10.1016/j.seares.2015.02.007

Ducrotoy, J. P., & Elliott, M. (2008). The science and management of the North Sea and the Baltic Sea: Natural history, present threats and future challenges. *Marine Pollution Bulletin*, *57*(1–5), 8–21. https://doi.org/10.1016/j.marpolbul.2008.04.030

Ducrotoy, J.-P., Elliott, M., & de Jonge, V. N. (2000). The North Sea. *Marine Pollution Bulletin*, *41*(1–6), 5–23. https://doi.org/10.1016/S0025-326X(00)00099-0

Edwards, M., Beaugrand, G., Reid, P. C., Rowden, A. A., & Jones, M. B. (2002). Ocean climate anomalies and the ecology of the North Sea. *Marine Ecology Progress Series*, *239*, 1–10. https://doi.org/10.3354/MEPS239001

Emeis, K. C., van Beusekom, J., Callies, U., Ebinghaus, R., Kannen, A., Kraus, G., Kröncke, I., Lenhart, H., Lorkowski, I., Matthias, V., Möllmann, C., Pätsch, J., Scharfe, M., Thomas, H., Weisse, R., & Zorita, E. (2015). The North Sea - A shelf sea in the Anthropocene. *Journal of Marine Systems*, *141*, 18–33. https://doi.org/10.1016/j.jmarsys.2014.03.012

Ferreira, J. G., Andersen, J. H., Borja, A., Bricker, S. B., Camp, J., Cardoso da Silva, M., Garcés, E., Heiskanen, A. S., Humborg, C., Ignatiades, L., Lancelot, C., Menesguen, A., Tett, P., Hoepffner, N., & Claussen, U. (2011). Overview of eutrophication indicators to assess environmental status within the European Marine Strategy Framework Directive. *Estuarine, Coastal and Shelf Science*, *93*(2), 117–131. https://doi.org/10.1016/j.ecss.2011.03.014

Gholizadeh, M., Melesse, A., & Reddi, L. (2016). A Comprehensive Review on Water Quality Parameters Estimation Using Remote Sensing Techniques. *Sensors*, *16*(8), 1298. https://doi.org/10.3390/s16081298

Gypens, N., Borges, A. V., & Lancelot, C. (2009). Effect of eutrophication on air-sea CO<inf>2</inf> fluxes in the coastal Southern North Sea: A model study of the past 50 years. *Global Change Biology*, *15*(4), 1040–1056. https://doi.org/10.1111/j.1365-2486.2008.01773.x

Gypens, Nathalie, Lacroix, G., & Lancelot, C. (2007). Causes of variability in diatom and Phaeocystis blooms in Belgian coastal waters between 1989 and 2003: A model study. *Journal of Sea Research*, *57*(1), 19–35. https://doi.org/10.1016/J.SEARES.2006.07.004

Hernández-Fariñas, T., Soudant, D., Barillé, L., Belin, C., Lefebvre, A., & Bacher, C. (2014). Temporal changes in the phytoplankton community along the French coast of the eastern English Channel and the southern Bight of the North Sea. *ICES Journal of Marine Science*, *71*(4), 821–833. https://doi.org/10.1093/ICESJMS/FST192

Høyer, J. L., & Karagali, I. (2016). Sea Surface Temperature Climate Data Record for the North Sea and Baltic Sea. *Journal of Climate*, *29*(7), 2529–2541. https://doi.org/10.1175/JCLI-D-15-0663.1

Hunter-Cevera, K. R., Neubert, M. G., Olson, R. J., Solow, A. R., Shalapyonok, A., & Sosik, H. M. (2016). Physiological and ecological drivers of early spring blooms of a coastal phytoplankter. *Science*, *354*(6310), 326–329. https://doi.org/10.1126/SCIENCE.AAF8536

IOCCG. (2000). IOCCG Report Number 03: Remote Sensing of Ocean Colour in Coastal, and Other Optically-Complex, Waters. *IOCCG Web Page*, *3*(October), 1–145. http://www.vliz.be/imis/imis.php?module=ref&refid=134621&request=147862

Istvánovics, V. (2009). Eutrophication of Lakes and Reservoirs. *Encyclopedia of Inland Waters*, 157–165. https://doi.org/10.1016/B978-012370626-3.00141-1

Joint, I., & Pomroy, A. (1993). Phytoplankton biomass and production in the southern North Sea. *Marine Ecology Progress Series*, *99*(1–2), 169–182. https://doi.org/10.3354/meps099169

Karydis, Michael, & Kitsiou, D. (2014). Eutrophication in the european regional seas: A review on impacts, assessment and policy. In *Phytoplankton: Biology, Classification and Environmental Impacts* (pp. 167–243). Nova Science Publishers, Inc.

Kitsiou, D., & Karydis, M. (2011). Coastal marine eutrophication assessment: A review on data analysis. In *Environment International* (Vol. 37, Issue 4, pp. 778–801). Elsevier Ltd. https://doi.org/10.1016/j.envint.2011.02.004

Lancelot, C, Spitz, Y., Gypens, N., Ruddick, K., Becquevort, S., Rousseau, V., Lacroix, G., & Billen, G. (2005). Modelling diatom and Phaeocystis blooms and nutrient cycles in the Southern Bight of the North Sea: the MIRO model. *Marine Ecology Progress Series*, *289*, 63–78. https://doi.org/10.3354/meps289063

Lancelot, Chrisitane, Rousseau, V., Billen, G., & van Eeckhout, D. (1997). 4. Coastal eutrophication of the Southern Bight of the North Sea: Assessment and modelling. *Bulletin de La Societe Royale Des Sciences de Liege*, *66*(1–3), 27–38. https://doi.org/10.1007/978-94-011-5758-2_33

Lancelot, Christiane, Rousseau, V., & Gypens, N. (2009). Ecologically based indicators for Phaeocystis disturbance in eutrophied Belgian coastal waters (Southern North Sea) based on field observations and ecological modelling. *Journal of Sea Research*, *61*(1–2), 44–49. https://doi.org/10.1016/J.SEARES.2008.05.010

Lavigne, H., van der Zande, D., Ruddick, K., Cardoso Dos Santos, J. F., Gohin, F., Brotas, V., & Kratzer, S. (2021). Quality-control tests for OC4, OC5 and NIR-red satellite chlorophyll-a algorithms applied to coastal waters. *Remote Sensing of Environment*, *255*, 112237. https://doi.org/10.1016/J.RSE.2020.112237

Lenhart, H. J., Mills, D. K., Baretta-Bekker, H., van Leeuwen, S. M., der Molen, J. van, Baretta, J. W., Blaas, M., Desmit, X., Kühn, W., Lacroix, G., Los, H. J., Ménesguen, A., Neves, R., Proctor, R., Ruardij, P., Skogen, M. D., Vanhoutte-Brunier, A., Villars, M. T., & Wakelin, S. L. (2010). Predicting the consequences of nutrient reduction on the eutrophication status of the North Sea. *Journal of Marine Systems*, *81*(1–2), 148–170. https://doi.org/10.1016/j.jmarsys.2009.12.014

Leynaert, V. R. A., Daoud, N., & Lancelot, C. (2002). Diatom succession, silicification and silicic acid availability in Belgian coastal waters (Southern North Sea). *Marine Ecology Progress Series*, *236*, 61–73. https://doi.org/10.3354/MEPS236061

Llope, M., Chan, K. S., Ciannelli, L., Reid, P. C., Stige, L. C., & Stenseth, N. C. (2009). Effects of environmental conditions on the seasonal distribution of phytoplankton biomass in the North Sea. *Limnology and Oceanography*, *54*(2), 512–524. https://doi.org/10.4319/LO.2009.54.2.0512

Llort, J., Lévy, M., Sallée, J.-B., & Tagliabue, A. (2015). Onset, intensification, and decline of phytoplankton blooms in the Southern Ocean. *ICES Journal of Marine Science*, *72*(6), 1971–1984. https://doi.org/10.1093/icesjms/fsv053

Lohmann, G., & Wiltshire, K. H. (2012). Winter atmospheric circulation signature for the timing of the spring bloom of diatoms in the North Sea. *Marine Biology 2012 159:11*, *159*(11), 2573–2581. https://doi.org/10.1007/S00227-012-1993-7

Matthews, M. W., & Bernard, S. (2015). Eutrophication and cyanobacteria in South Africa's standing water bodies: A view from space. *South African Journal of Science*, *111*(5–6), 1–8. https://doi.org/10.17159/sajs.2015/20140193

McQuatters-Gollop, A., Raitsos, D. E., Edwards, M., Pradhan, Y., Mee, L. D., Lavender, S. J., & Attrill, M. J. (2007). A long-term chlorophyll data set reveals regime shift in North Sea phytoplankton biomass unconnected to nutrient trends. *Limnology and Oceanography*, *52*(2), 635–648. https://doi.org/10.4319/lo.2007.52.2.0635

Muylaert, K., Gonzales, R., Franck, M., Lionard, M., van der Zee, C., Cattrijsse, A., Sabbe, K., Chou, L., & Vyverman, W. (2006). Spatial variation in phytoplankton dynamics in the Belgian coastal zone of the North Sea studied by microscopy, HPLC-CHEMTAX and underway fluorescence recordings. *Journal of Sea Research*, *55*(4), 253–265. https://doi.org/10.1016/j.seares.2005.12.002

Nechad, B., Ruddick, K. G., & Park, Y. (2010). Calibration and validation of a generic multisensor algorithm for mapping of total suspended matter in turbid waters. *Remote Sensing of Environment*, *114*(4), 854–866. https://doi.org/10.1016/J.RSE.2009.11.022

Nohe, Anja, Goffin, A., Tyberghein, L., Lagring, R., de Cauwer, K., Vyverman, W., & Sabbe, K. (2020). Marked changes in diatom and dinoflagellate biomass, composition and seasonality in the Belgian Part of the North Sea between the 1970s and 2000s. *Science of the Total Environment*, *716*, 136316. https://doi.org/10.1016/j.scitotenv.2019.136316

Opdal, A. F., Lindemann, C., & Aksnes, D. L. (2019). Centennial decline in North Sea water clarity causes strong delay in phytoplankton bloom timing. *Global Change Biology*, *25*(11), 3946–3953. https://doi.org/10.1111/gcb.14810

Otto, L., Zimmerman, J. T. F., Furnes, G. K., Mork, M., Saetre, R., & Becker, G. (1990). Review of the physical oceanography of the North Sea. *Netherlands Journal of Sea Research*, *26*(2–4), 161. https://doi.org/10.1016/0077-7579(90)90091-T

Passy, P., Gypens, N., Billen, G., Garnier, J., Thieu, V., Rousseau, V., Callens, J., Parent, J. Y., & Lancelot, C. (2013). A model reconstruction of riverine nutrient fluxes and eutrophication in the Belgian Coastal Zone since 1984. *Journal of Marine Systems*, *128*, 106–122. https://doi.org/10.1016/j.jmarsys.2013.05.005

Peeters, F., Straile, D., Lorke, A., & Livingstone, D. M. (2007). Earlier onset of the spring phytoplankton bloom in lakes of the temperate zone in a warmer climate. *Global Change Biology*, *13*(9), 1898–1909. https://doi.org/10.1111/J.1365-2486.2007.01412.X

Peperzak, L., & Witte, H. (2019). Abiotic drivers of interannual phytoplankton variability and a 1999–2000 regime shift in the North Sea examined by multivariate statistics. *Journal of Phycology*, *55*(6), 1274–1289. https://doi.org/10.1111/JPY.12893

Philippart, C. J. M., van Iperen, J. M., Cadée, G. C., & Zuur, A. F. (2010). Long-term field observations on seasonality in chlorophyll-a concentrations in a shallow coastal marine ecosystem, the Wadden Sea. *Estuaries and Coasts*, *33*(2), 286–294. https://doi.org/10.1007/s12237-009-9236-y

Prins, T. C., Desmit, X., & Baretta-Bekker, J. G. (2012). Phytoplankton composition in Dutch coastal waters responds to changes in riverine nutrient loads. *Journal of Sea Research*, *73*, 49–62. https://doi.org/10.1016/J.SEARES.2012.06.009

Reid, P. C., Lancelot, C., Gieskes, W. W. C., Hagmeier, E., & Weichart, G. (1990). Phytoplankton of the North Sea and its dynamics: A review. *Netherlands Journal of Sea Research*, *26*(2–4), 295–331. https://doi.org/10.1016/0077-7579(90)90094-W

Rousseau, V., Lancelot, C., & Cox, D. (2008). *Current Status of Eutrophication in the Belgian Coastal Zone*. https://doi.org/O

Rousseau, Véronique, Lantoine, F., Rodriguez, F., LeGall, F., Chrétiennot-Dinet, M. J., & Lancelot, C. (2013). Characterization of Phaeocystis globosa (Prymnesiophyceae), the blooming species in the Southern North Sea. *Journal of Sea Research*, *76*, 105–113. https://doi.org/10.1016/j.seares.2012.07.011

Ruddick, K., Lacroix, G., Lancelot, C., Nechad, B., Park, Y., Peters, S., & van Mol, B. (2008). Optical remote sensing of the north sea. In *Remote Sensing of the European Seas* (pp. 79–90). Springer Netherlands. https://doi.org/10.1007/978-1-4020-6772-3_6

Scharfe, M., & Wiltshire, K. H. (2019). Modeling of intra-annual abundance distributions: Constancy and variation in the phenology of marine phytoplankton species over five decades at Helgoland Roads (North Sea). *Ecological Modelling*, *404*, 46–60. https://doi.org/10.1016/J.ECOLMODEL.2019.01.001

Sharples, J., Ross, O. N., Scott, B. E., Greenstreet, S. P. R., & Fraser, H. (2006). Inter-annual variability in the timing of stratification and the spring bloom in the North-western North Sea. *Continental Shelf Research*, *26*(6), 733–751. https://doi.org/10.1016/J.CSR.2006.01.011

Sommer, U., & Lewandowska, A. (2011). Climate change and the phytoplankton spring bloom: warming and overwintering zooplankton have similar effects on phytoplankton. *Global Change Biology*, *17*(1), 154–162. https://doi.org/10.1111/J.1365-2486.2010.02182.X

Speeckaert, G., Borges, A. v., Champenois, W., Royer, C., & Gypens, N. (2018). Annual cycle of dimethylsulfoniopropionate (DMSP) and dimethylsulfoxide (DMSO) related to phytoplankton succession in the Southern North Sea. *Science of the Total Environment*, *622–623*, 362–372. https://doi.org/10.1016/j.scitotenv.2017.11.359

Sündermann, J., & Pohlmann, T. (2011). A brief analysis of North Sea physics. In *Oceanologia* (Vol. 53, Issue 3, pp. 663–689). Polish Academy of Sciences. https://doi.org/10.5697/oc.53-3.663

Thomas, Y., Cassou, C., Gernez, P., & Pouvreau, S. (2018). Oysters as sentinels of climate variability and climate change in coastal ecosystems. *Environmental Research Letters*, *13*(10). https://doi.org/10.1088/1748-9326/aae254

Ueyama, R., & Monger, B. C. (2005). Wind-induced modulation of seasonal phytoplankton blooms in the North Atlantic derived from satellite observations. *Limnology and Oceanography*, *50*(6), 1820–1829. https://doi.org/10.4319/LO.2005.50.6.1820

van Aken, H. M. (2010). Meteorological forcing of long-term temperature variations of the Dutch coastal waters. *Journal of Sea Research*, *63*(2), 143–151. https://doi.org/10.1016/J.SEARES.2009.11.005

van der Zande, D., Lacroix, G., & Ruddick, K. (2012). Observing and Explaining the Timing of Spring/Summer Algal Blooms in the Southern North Sea Using Ocean Colour Remote Sensing. *Proceedings of the Ocean Optics XXI Conference*.

van der Zande, D., Lavigne, H., Blauw, A., Prins, T., Desmit, X., Eleveld, M., Gohin, F., Pardo, S., Tilstone, G., & Cardoso Dos Santos, J. (2019). *Coherence in assessment framework of chlorophyll a and nutrients as part of the EU project 'Joint monitoring programme of the eutrophication of the North Sea with satellite data' (Ref: DG ENV/MSFD Second Cycle/2016)*. (Issue Activity 2).

Weijerman, M., Lindeboom, H., & Zuur, A. F. (2005). Regime shifts in marine ecosystems of the North Sea and Wadden Sea. *Marine Ecology Progress Series*, *298*, 21–39. https://doi.org/10.3354/MEPS298021

Weisse, T., Tande, K., Verity, P., Hansen, F., & Gieskes, W. (1994). The trophic significance of Phaeocystis blooms. *Journal of Marine Systems*, *5*(1), 67–79. https://doi.org/10.1016/0924-7963(94)90017-5

Wilson, R. J., & Heath, M. R. (2019). Increasing turbidity in the North Sea during the 20th century due to changing wave climate. *Ocean Science*, *15*(6), 1615–1625. https://doi.org/10.5194/OS-15-1615-2019

Wiltshire, Karen H., Boersma, M., Carstens, K., Kraberg, A. C., Peters, S., & Scharfe, M. (2015). Control of phytoplankton in a shelf sea: Determination of the main drivers based on the Helgoland Roads Time Series. *Journal of Sea Research*, *105*, 42–52. https://doi.org/10.1016/J.SEARES.2015.06.022

Wiltshire, Karen H., & Manly, B. F. J. (2004). The warming trend at Helgoland Roads, North Sea: phytoplankton response. *Helgoland Marine Research 2004 58:4*, *58*(4), 269–273. https://doi.org/10.1007/S10152-004-0196-0

Wiltshire, Karen Helen, Kraberg, A., Bartsch, I., Boersma, M., Franke, H.-D., Freund, J., Gebühr, C., Gerdts, G., Stockmann, K., & Wichels, A. (2009). Helgoland Roads, North Sea: 45 Years of Change. *Estuaries and Coasts 2009 33:2*, *33*(2), 295–310. https://doi.org/10.1007/S12237-009-9228-Y

Winder, M., & Sommer, U. (2012). Phytoplankton response to a changing climate. *Hydrobiologia 2012 698:1*, *698*(1), 5–16. https://doi.org/10.1007/S10750-012-1149-2

Xu, X., Lemmen, C., & Wirtz, K. W. (2020). Less Nutrients but More Phytoplankton: Long-Term Ecosystem Dynamics of the Southern North Sea. *Frontiers in Marine Science*, *7*, 662. https://doi.org/10.3389/fmars.2020.00662

Zhai, L., Platt, T., Tang, C., Sathyendranath, S., & Walne, A. (2013). The response of phytoplankton to climate variability associated with the North Atlantic Oscillation. *Deep Sea Research Part II: Topical Studies in Oceanography*, *93*, 159–168. https://doi.org/10.1016/J.DSR2.2013.04.009